



**HAL**  
open science

## Magnetic moment estimation and bounded extremal problems

Laurent Baratchart, Sylvain Chevillard, Douglas P. Hardin, Juliette Leblond,  
Eduardo Andrade Lima, Jean-Paul Marmorat

► **To cite this version:**

Laurent Baratchart, Sylvain Chevillard, Douglas P. Hardin, Juliette Leblond, Eduardo Andrade Lima, et al.. Magnetic moment estimation and bounded extremal problems. *Inverse Problems and Imaging*, In press. hal-01623991v1

**HAL Id: hal-01623991**

**<https://inria.hal.science/hal-01623991v1>**

Submitted on 26 Oct 2017 (v1), last revised 10 Dec 2018 (v2)

**HAL** is a multi-disciplinary open access archive for the deposit and dissemination of scientific research documents, whether they are published or not. The documents may come from teaching and research institutions in France or abroad, or from public or private research centers.

L'archive ouverte pluridisciplinaire **HAL**, est destinée au dépôt et à la diffusion de documents scientifiques de niveau recherche, publiés ou non, émanant des établissements d'enseignement et de recherche français ou étrangers, des laboratoires publics ou privés.

# Magnetic moment estimation and bounded extremal problems

Laurent Baratchart\*   Sylvain Chevillard\*   Douglas Hardin<sup>†</sup>  
Juliette Leblond\*   Eduardo Andrade Lima<sup>‡</sup>   Jean-Paul Marmorat<sup>§</sup>

October 25, 2017

## Abstract

We consider the inverse problem in magnetostatics for recovering the moment of a planar magnetization from measurements of the normal component of the magnetic field at a distance from the support. Such issues arise in studies of magnetic material in general and in paleomagnetism in particular. Assuming the magnetization is a measure with  $L^2$ -density, we construct linear forms to be applied on the data in order to estimate the moment. These forms are obtained as solutions to certain extremal problems in Sobolev classes of functions, and their computation reduces to solving an elliptic differential-integral equation, for which synthetic numerical experiments are presented.

## 1 Introduction

In this paper, we study a family of constrained best-approximation problems in certain Hilbert spaces of harmonic gradients, which are motivated by inverse magnetization problems arising in geosciences and planetary sciences. The physical setting, along with instrumentation issues and related questions from paleomagnetism, are described in the introductory sections of [5, 6, 7, 20] to which this work may be viewed as a sequel. The goal is to analyze magnetized thin rock samples carrying some unknown magnetization distribution to be estimated from measurements of the magnetic field. Specifically, a sample  $\mathbf{S}$  is identified with a compact subset of a plane  $P_0 \subset \mathbb{R}^3$ , and is assumed to support a  $\mathbb{R}^3$ -valued magnetization distribution  $\mathbf{m}$ . The measurements consist of pointwise values, on a compact set  $\mathbf{Q}$  contained in a plane  $P_h$  parallel to  $P_0$  lying at distance  $h > 0$  from it, of the normal component of the magnetic field produced by  $\mathbf{m}$  (normal to  $P_h$ , that is). For definiteness, we assume that both  $\mathbf{S}$  and  $\mathbf{Q}$  are compact rectangles, centered at the origin, in the horizontal planes  $\mathbb{R}^2 \times \{0\} \subset \mathbb{R}^3$  and  $\mathbb{R}^2 \times \{h\}$ , respectively. Thus, the measured quantity is the vertical component  $b_3[\mathbf{m}]$  of the magnetic field produced by  $\mathbf{m}$ ,

---

\*Team APICS, INRIA, BP 93, 06902 Sophia Antipolis Cedex, France.

<sup>†</sup>Department of Mathematics, Vanderbilt University, Nashville, TN 37240, USA.

<sup>‡</sup>Department of Earth, Atmospheric and Planetary Sciences, MIT, Cambridge, MA 02139, USA.

<sup>§</sup>Center of Applied Mathematics, Ecole des Mines ParisTech, CS 10 207, 06904 Sophia Antipolis Cedex, France.

31 evaluated on  $\mathbf{Q}$ . Maxwell's equations for the magnetostatic case [15, Ch. 5] imply that  
 32 this magnetic field derives from a scalar magnetic potential  $\Lambda$  which is a solution to the  
 33 Poisson equation  $\Delta\Lambda = \operatorname{div} \mathbf{m}$  in  $\mathbb{R}^3$ . Consequently, we have that  $b_3[\mathbf{m}] = -\mu_0 \partial_{x_3}\Lambda$  with  
 34  $\mu_0 = 4\pi \times 10^{-7}$ , see *e.g.* [7, 5].

35 It is well-known that some magnetizations generate no external magnetic field (*i.e.*,  
 36 the zero field): these are called silent. A description of silent magnetization distributions  
 37 supported in a plane is given in [7], under weak assumptions on the distribution. In  
 38 particular, those having compact support admit a simple characterization, *cf.* Section 2.2.  
 39 Moreover, it is shown in [5] that if the normal component of the field vanishes everywhere on  
 40 an open subset of a plane, then the field is identically zero and therefore the magnetization  
 41 is silent. Thus, with the previous notation, it holds that  $b_3[\mathbf{m}] = 0$  on  $\mathbf{Q}$  if and only if  $\mathbf{m}$   
 42 is a silent magnetization of the type described in [7]. The existence of such magnetizations  
 43 is a major obstacle for solving the inverse magnetization problem, for it implies that  
 44 additional assumptions must be made to achieve full recovery. In the present work, we  
 45 focus on a much simpler inverse problem, which consists in estimating the net moment  
 46  $\langle \mathbf{m} \rangle$  of the unknown magnetization  $\mathbf{m}$ , *i.e.* the integral of  $\mathbf{m}^1$ . So, we merely aim at  
 47 recovering a vector in  $\mathbb{R}^3$  (namely  $\langle \mathbf{m} \rangle$ ) rather than the whole distribution  $\mathbf{m}$  on the  
 48 rectangle  $\mathbf{S}$ . Unlike magnetization recovery, net moment recovery is meaningful without  
 49 extra-assumptions on  $\mathbf{m}$ , because silent magnetizations are easily seen to have zero  
 50 moment.

51 Though much less ambitious than solving the full inverse magnetization problem,  
 52 determining the net moment is still a significant goal. Indeed, classical magnetometers  
 53 estimate the net moment of a sample by comparing it to a dipolar source, an approximation  
 54 which is valid at a distance from the sample only. When dealing with weakly magnetized  
 55 objects, the field away from the sample gets too small and is easily dominated by other,  
 56 spurious magnetic sources, so that measurements by standard magnetometers may become  
 57 unreliable. This is a typical issue in paleomagnetism, which justifies our present attempt to  
 58 devise algorithms to estimate the moment from measurements of (the vertical component  
 59 of) the field, close to the sample. Such measurements can be performed by very sensitive  
 60 instruments known as Scanning QUantum Interference Device (SQUID) microscopes,  
 61 see [7, 20] for more explanation.

62 From a physical viewpoint, knowing the net moment of a magnetization  $\mathbf{m}$  is a basic  
 63 piece of information that is relevant in itself. It gains further significance when putting  
 64 additional assumptions on  $\mathbf{m}$ , assuming for instance that it is unidimensional (*i.e.* that it  
 65 takes values in a 1-dimensional subspace of  $\mathbb{R}^3$ ). Unidimensionality is a fairly common  
 66 assumption in paleomagnetism, at least for igneous rocks that cooled down in the presence  
 67 of an ambient field during formation and whose remanent magnetization keeps record  
 68 of the strength and direction of that field. Clearly, if a magnetization is unidimensional  
 69 then its direction must be the one of the net moment. Now, if we are able to compute  
 70 this moment, one may consider rather efficient regularizing techniques in the Fourier  
 71 domain to recover it, see [20] and [7, Sec. 4.1]. More can be said in this connection: in  
 72 fact, to *any* magnetization  $\mathbf{m}$  compactly supported in a plane, there is a unidimensional  
 73 magnetization  $\mathbf{u}$  supported on the same plane which generates the *same* field on a given  
 74 connected component of the complement of the measurement plane. Surprisingly perhaps,

---

<sup>1</sup>Mathematically speaking,  $\langle \mathbf{m} \rangle$  is the effect of the distribution  $\mathbf{m}$  on any smooth compactly supported function on  $\mathbb{R}^3$  which is identically 1 in a neighborhood of  $\mathbf{S}$ , see Section 2.2.

75 the direction of  $\mathbf{u}$  can even be picked arbitrarily provided it is not tangent to the plane [7,  
76 Thm 3.6]; however, clearly,  $\mathbf{u}$  will not have the same support as  $\mathbf{m}$  in general, and will  
77 typically be non-compactly supported. Now, even in this case, choosing  $\mathbf{u}$  to have the  
78 direction of  $\langle \mathbf{m} \rangle$  has a regularizing effect on the Fourier techniques just mentioned, because  
79 the singularity of the Fourier transform  $\hat{\mathbf{u}}$  at 0 can then be singled out explicitly, compare  
80 [7, Eqns (29)-(30)]. This dangles the prospect of efficiently computing a unidimensional  
81 magnetization which differs from the true one by a (generally non-compactly supported)  
82 silent magnetization. Because the latter can be characterized completely, estimating the  
83 net moment may thus be envisaged as an initial step to study the inverse magnetization  
84 problem in general.

85 Having made the case for net moment recovery and pointed out that it was an easier  
86 task than full inversion, we should nevertheless stress that it is nontrivial. A main reason  
87 is that measurements of  $b_3[\mathbf{m}]$  are taken merely on  $\mathbf{Q}$  which does not surround  $\mathbf{S}$ . If  
88 measurements were available on the entire plane  $\mathbb{R}^2 \times \{h\}$  (which does surround  $\mathbf{S}$  if  
89 one takes into account points at infinity), then asymptotic formulas from [6] would allow  
90 us in principle to approximate the net moment arbitrary well, at least if  $\mathbf{m}$  is smooth  
91 enough, say if it is a measure. However, the fact that measurements are available on  $\mathbf{Q}$   
92 only makes the problem ill-posed, in that small differences in  $b_3[\mathbf{m}]$  on  $\mathbf{Q}$  may result in  
93 large differences on  $\langle \mathbf{m} \rangle$ , *cf.* Section 2.2. This is precisely the issue that we address in the  
94 present work. Further reasons why net moment recovery is difficult in practice lie with  
95 the presence of noise in the measurements, inherent in such problems. In this paper, we  
96 only deal with synthetic examples corrupted by a small additive Gaussian white noise,  
97 and we do not touch upon this important facet of the situation except for some general  
98 comments in Sections 2.3 and 5.2.

99 We shall restrict ourselves to the elementary case where  $\mathbf{m}$  is a measure supported  
100 on  $\mathbf{S}$  with square summable density there. This makes for a Hilbertian framework which  
101 keeps the analysis simple. Hopefully this case is already typical of the main features of our  
102 method, though there is grounds to develop a similar approach in non Hilbertian contexts,  
103 for instance when magnetizations are measures normed with the total variation. Roughly  
104 speaking, what we do in this paper is to construct a  $\mathbb{R}^3$ -valued function  $\phi$  on  $\mathbf{Q}$  such that

$$\iint_{\mathbf{Q}} b_3[\mathbf{m}] \phi \sim \iint_{\mathbf{S}} \mathbf{m} = \langle \mathbf{m} \rangle \quad (1)$$

105 for all  $\mathbf{m} \in L^2(\mathbf{S}, \mathbb{R}^3)$  of given norm, with a bound on the norm of the derivative of  $\phi$  in  
106  $L^2(\mathbf{Q}, \mathbb{R}^{3 \times 2})$  which serves as a regularization parameter. In other words, we construct a  
107 linear estimator  $\phi$  to be applied to the data  $b_3[\mathbf{m}]$  for estimating  $\langle \mathbf{m} \rangle$ , but a trade-off  
108 exists between quality of approximation in (1) and oscillation of  $\phi$ . Note that oscillatory  
109 behavior is undesirable to evaluate the left hand side of (1) from pointwise values of  $b_3[\mathbf{m}]$   
110 with good accuracy. Besides, our choice to bound the derivative of  $\phi$  makes for an easy  
111 theoretical solution of the extremal problems involved in our analysis.

112 To conclude this introduction, let us mention also that when  $\mathbf{m}$  is the sum of several  
113 magnetization distributions with disjoint supports, then the individual moment of a  
114 component can be estimated even though we measure the global field, provided we have  
115 *a priori* knowledge of a neighborhood of the support of that component that does not  
116 intersect the support of any other. This can be done by essentially the same techniques  
117 as those we use to get (1). Computing such local moments could be of interest to

118 get information on the support of  $\mathbf{m}$ , for instance to confirm that a region where no  
 119 magnetization is expected has indeed zero or near-zero moment.

120 The outline of this work is as follows. Section 2 is devoted to notation, definitions  
 121 and preliminaries, including a description of the net magnetic moment recovery problem.  
 122 This issue is recast in Section 3 as a bounded extremal problem for which existence and  
 123 uniqueness results are proven. A characterization of the solution in terms of a critical  
 124 point equation involving a Lagrange parameter is then derived. Two methods for solving  
 125 the critical point equation numerically are presented in Section 4, one of which is used in  
 126 Section 5 to provide numerical illustrations. Section 6 has concluding remarks.

## 127 2 Notation and preliminaries

### 128 2.1 Function spaces

129 For  $\mathbf{x} = (x_1, \dots, x_n)^t \in \mathbb{R}^n$ , we let  $\|\mathbf{x}\| = (x_1^2 + \dots + x_n^2)^{1/2}$  be its Euclidean norm; here  
 130 and below, a superscript “ $t$ ” means “transpose”. Denote the scalar product of  $\mathbf{x}$  and  $\mathbf{y}$  by  
 131  $\mathbf{x} \cdot \mathbf{y} = \sum_j x_j y_j$ . The notation stands irrespective of  $n$  but no confusion should arise, and  
 132 we are only concerned with  $n = 2, 3$ . We write  $\bar{E}$  for the closure of a set  $E$  and for  $n = 2$   
 133 we indicate the open disk of center  $\mathbf{x}$  and radius  $R$  with  $D(\mathbf{x}, R)$ .

134 We write  $C^\infty(\Omega)$  for the space of smooth functions on an open set  $\Omega \subset \mathbb{R}^n$  having  
 135 continuous derivatives of any order, and  $C_0^\infty(\Omega)$  for the space of smooth functions with  
 136 compact support in  $\Omega$ . Recall that distributions on  $\Omega$  are linear forms on  $C_0^\infty(\Omega)$  which  
 137 are continuous for a certain topology, the precise definition of which may be found in [22,  
 138 Sec. I.2]. The support of a distribution  $\mathfrak{d}$  on  $\Omega$ , denoted by  $\text{supp } \mathfrak{d}$ , is the largest closed  
 139 set  $E \subset \Omega$  such that  $\mathfrak{d}(\varphi) = 0$  for all  $\varphi \in C_0^\infty(\Omega \setminus E)$ .

140 Distributions get differentiated by the usual rule:  $\partial_{x_i} \mathfrak{d}(\varphi) = -\mathfrak{d}(\partial_{x_i} \varphi)$ , with  $\partial_{x_i}$  to  
 141 mean the partial derivative with respect to the coordinate  $x_i$ . It is standard to regard  
 142 locally integrable functions as distributions by putting  $\psi(\varphi) = \int \psi \varphi$ . For  $\phi$  a distribution  
 143 or a function, we let  $\nabla \phi = (\partial_{x_1} \phi, \dots, \partial_{x_n} \phi)^t$  for the gradient of  $\phi$ . The divergence  
 144 operator, which is the distributional adjoint to  $\nabla$ , is denoted as  $\nabla \cdot$  and acts on  $\mathbb{R}^n$ -valued  
 145 distributions as  $\nabla \cdot (\phi_1, \dots, \phi_n) = \sum_{1 \leq j \leq n} \partial_{x_j} \phi_j$ . The Laplace operator  $\Delta$  is defined by  
 146  $\Delta \phi = \sum_{1 \leq j \leq n} \partial_{x_j}^2 \phi$ . These operator notations stand irrespective of  $n$ , but no confusion  
 147 should arise. In fact we use them for  $n = 2$ , except in Equation (4) when we introduce  
 148 the magnetic potential in general form, and after Equation (10) when we introduce silent  
 149 magnetizations.

150 We need some standard functions spaces but only in dimension two, so we restrict the  
 151 discussion to this case. For  $\Omega \subseteq \mathbb{R}^2$ , we denote by  $L^2(\Omega, \mathbb{R}^k)$  the familiar Lebesgue space  
 152 of  $\mathbb{R}^k$ -valued square summable functions which is a Hilbert space with norm and scalar  
 153 product:

$$\|\phi\|_{L^2(\Omega, \mathbb{R}^k)}^2 := \int_{\Omega} \|\phi\|^2 d\ell, \quad \langle \phi, \psi \rangle_{L^2(\Omega, \mathbb{R}^k)} := \int_{\Omega} \phi \cdot \psi d\ell,$$

154 with  $d\ell$  to indicate Lebesgue measure. We simply write  $L^2(\Omega)$  if  $k = 1$ . If  $\Omega$  is open, we  
 155 put  $W^{1,2}(\Omega)$  for the standard Sobolev space of functions belonging to  $L^2(\Omega)$  together with  
 156 their first distributional derivatives. It is a Hilbert space with norm:

$$\|\phi\|_{W^{1,2}(\Omega)}^2 = \|\phi\|_{L^2(\Omega)}^2 + \|\nabla \phi\|_{L^2(\Omega, \mathbb{R}^2)}^2.$$

157 We let  $W_0^{1,2}(\Omega)$  be the closure of  $C_0^\infty(\Omega)$  in  $W^{1,2}(\Omega)$ . If  $\Omega$  is bounded, the Sobolev-  
 158 Poincaré inequality [8, Cor. 9.19] implies there exists a constant  $C > 0$  (depending on  $\Omega$ )  
 159 such that

$$\|\phi\|_{L^2(\Omega)} \leq C \|\nabla \phi\|_{L^2(\Omega, \mathbb{R}^2)}, \quad \forall \phi \in W_0^{1,2}(\Omega). \quad (2)$$

160 Therefore  $\|\cdot\|_{W^{1,2}(\Omega)}$  and  $\|\nabla \cdot\|_{L^2(\Omega, \mathbb{R}^2)}$  are equivalent norms on  $W_0^{1,2}(\Omega)$ , namely:

$$\|\nabla u\|_{L^2(\Omega, \mathbb{R}^2)} \leq \|u\|_{W^{1,2}(\Omega)} \leq \sqrt{C^2 + 1} \|\nabla u\|_{L^2(\Omega, \mathbb{R}^2)}, \quad u \in W_0^{1,2}(\Omega). \quad (3)$$

When  $\Omega$  is bounded and Lipschitz-smooth, meaning that its boundary  $\partial\Omega$  is locally the graph of a Lipschitz function, then functions in  $W^{1,2}(\Omega)$  have a trace on  $\partial\Omega$  which belongs to the fractional Sobolev space  $W^{1/2,2}(\partial\Omega)$ , consisting of square summable functions  $g$  with respect to arclength on  $\partial\Omega$  for which

$$\|g\|_{W^{1/2,2}(\partial\Omega)} = \|g\|_{L^2(\partial\Omega)} + \left( \int_{\partial\Omega \times \partial\Omega} \frac{|g(t) - g(t')|^2}{\|t - t'\|^2} |dt| |dt'| \right)^{1/2} < +\infty,$$

where  $|dt|$  indicates (the differential of) arclength. The trace operator is continuous and surjective onto  $W^{1/2,2}(\partial\Omega)$ . Functions with zero trace are exactly those belonging to  $W_0^{1,2}(\Omega)$ , and they are also those whose extension by zero outside  $\Omega$  defines a function in  $W^{1,2}(\mathbb{R}^2)$ . We also make use of the fractional Sobolev space  $W^{3/2,2}(\Omega)$ . The latter consists of functions  $g \in W^{1,2}(\Omega)$ , each partial derivative of which satisfies:

$$\left( \int_{\Omega \times \Omega} \frac{|\partial_{x_i} g(\mathbf{x}) - \partial_{x_i} g(\mathbf{y})|^2}{\|\mathbf{x} - \mathbf{y}\|^3} d\mathbf{x} d\mathbf{y} \right)^{1/2} < +\infty, \quad i = 1, 2.$$

161 The Sobolev space  $W^{2,2}(\Omega)$ , consists of functions in  $L^2(\Omega)$  whose partial derivatives of  
 162 the first order lie in  $W^{1,2}(\Omega)$ . It is a Hilbert space with norm

$$\|\phi\|_{W^{2,2}(\Omega)}^2 = \|\phi\|_{L^2(\Omega)}^2 + \|\nabla \phi\|_{L^2(\Omega, \mathbb{R}^2)}^2 + \sum_{1 \leq i < j \leq 2} \left\| \partial_{x_i} \partial_{x_j} \phi \right\|_{L^2(\Omega)}^2.$$

163 For  $0 \leq \alpha < 1$ , we put  $C^\alpha(\Omega)$  for the space of Hölder continuous functions of exponent  $\alpha$   
 164 on  $\Omega$ . We refer to [1], [8, Ch. 9], [23, Ch. V, VI] for classical properties of Sobolev spaces.  
 165 When  $f$  is a function on  $\Omega$ , we denote by  $\tilde{f}$  the extension of  $f$  by zero outside  $\Omega$ . That is,  
 166  $\tilde{f}$  is equal to  $f$  on  $\Omega$  and to 0 elsewhere. We also use at places the symbol  $\vee$  to mean  
 167 concatenation with another function defined on  $\mathbb{R}^2 \setminus \Omega$ : for instance  $\tilde{f} = f \vee 0$ . Clearly,  
 168  $\|f\|_{L^2(\Omega)} = \|\tilde{f}\|_{L^2(\mathbb{R}^2)}$  and if  $f \in W_0^{1,2}(\Omega)$  then  $\tilde{f} \in W^{1,2}(\mathbb{R}^2)$ .

## 169 2.2 Operators involved

170 The magnetic potential associated with a magnetization, modeled as a compactly supported  
 171  $\mathbb{R}^3$ -valued distribution  $\mathbf{m}$  on  $\mathbb{R}^3$ , is given by

$$\Lambda(\mathbf{x}) = -\frac{1}{4\pi} \left\langle \nabla \cdot \mathbf{m}, \frac{1}{\|\cdot - \mathbf{x}\|} \right\rangle = \frac{1}{4\pi} \left\langle \mathbf{m}, \nabla \left( \frac{1}{\|\cdot - \mathbf{x}\|} \right) \right\rangle, \quad \mathbf{x} \in \mathbb{R}^3 \setminus \text{supp } \mathbf{m}, \quad (4)$$

172 where the brackets denote the duality pairing between distributions and  $C_0^\infty(\mathbb{R}^3)$ -functions.  
 173 Note that the formula makes sense because  $\mathbf{y} \rightarrow 1/\|\mathbf{y} - \mathbf{x}\|$  coincides with a  $C_0^\infty(\mathbb{R}^3)$ -  
 174 function on a neighborhood of  $\text{supp } \mathbf{m}$  when  $\mathbf{x} \notin \text{supp } \mathbf{m}$ . In the particular case where  $\mathbf{m}$

175 is a  $\mathbb{R}^3$ -valued measure supported on a compact subset  $\mathbf{S}$  of the horizontal plane  $\mathbb{R}^2 \times \{0\}$ ,  
 176 with density  $\mathbf{m} = (m_1, m_2, m_3)$  there, then we get that

$$\Lambda(\mathbf{x}) = \frac{1}{4\pi} \iint_{\mathbf{S}} \frac{\mathbf{m}(\mathbf{t}) \cdot (\mathbf{x} - \mathbf{t})}{\|\mathbf{x} - \mathbf{t}\|^3} d\ell(\mathbf{t}), \quad \mathbf{x} \in \mathbb{R}^3 \setminus \mathbf{S}. \quad (5)$$

177 Let  $P_{x_3}$  be the Poisson kernel of the upper half-space  $\{x_3 > 0\}$ , see *e.g.* [24, Ch. I]:

$$P_{x_3} : \mathbf{x} \mapsto \frac{x_3}{2\pi\|\mathbf{x}\|^3}. \quad (6)$$

178 On this half-space, the previous expression for  $\Lambda$  implies that it is half the convolution  
 179 over  $\mathbb{R}^2$  of  $P_{x_3}$  with the function  $R_1\widetilde{m}_1 + R_2\widetilde{m}_2 + \widetilde{m}_3$ , where  $R_1, R_2$  are the Riesz transforms  
 180 on  $\mathbb{R}^2$ , see [7, Sec. 2]). In other words, for  $x_3 > 0$ ,  $2\Lambda(x_3)$  is the harmonic extension of  
 181  $R_1\widetilde{m}_1 + R_2\widetilde{m}_2 + \widetilde{m}_3$  to the upper half space. Likewise, for  $x_3 < 0$ ,  $2\Lambda(x_3)$  is the harmonic  
 182 extension of  $R_1\widetilde{m}_1 + R_2\widetilde{m}_2 - \widetilde{m}_3$  to the lower half space.

183 Hereafter, we let  $S$  and  $Q$  be two Lipschitz-smooth bounded non-empty open sets  
 184 in  $\mathbb{R}^2 \times \{0\}$  and  $\mathbb{R}^2 \times \{h\}$  respectively. For simplicity, we also assume that  $S$  is simply  
 185 connected. One may think of  $S, Q$  as being rectangles whose closures  $\overline{S}, \overline{Q}$  are the sets  $\mathbf{S},$   
 186  $\mathbf{Q}$  introduced in Section 1. Observe that expression (5) for  $\Lambda$  may as well be computed  
 187 as an integral over  $S$  because the boundary  $\partial S = \mathbf{S} \setminus S$  has Lebesgue measure zero. We  
 188 often identify  $S$  and  $Q$  with subsets of  $\mathbb{R}^2$ , while the third component (0 in the case of  $S$   
 189 and  $h$  in the case of  $Q$ ) is treated as a parameter.

190 The main operator under consideration here is  $\mathbf{m} \rightarrow b_3[\mathbf{m}]$ , which maps the magne-  
 191 tization  $\mathbf{m} = (m_1, m_2, m_3) \in L^2(S, \mathbb{R}^3)$  to the vertical component of the magnetic field  
 192 on  $Q$ . Specifically,  $b_3 : L^2(S, \mathbb{R}^3) \rightarrow L^2(Q)$  is defined by

$$b_3[\mathbf{m}] = -\mu_0 \partial_{x_3} \Lambda, \quad x_3 = h. \quad (7)$$

193 Although the target space is here  $L^2(Q)$ , it is clear since  $h > 0$  that the range of  
 194  $b_3$  consists of restrictions to  $Q$  of smooth (even analytic) functions on  $\{x_3 > 0\}$ . Basic  
 195 properties of the operator  $b_3$  were given in [5, Sec. 3], [7]. Below, we recall some of them  
 196 that will be used in the course of the paper.

197

198 Recall the notation  $\widetilde{m}_i = m_i \vee 0 \in L^2(\mathbb{R}^2)$ . From the relation

$$\partial_{x_j} P_{x_3}(\mathbf{x}) = \partial_{x_j} \frac{x_3}{2\pi\|\mathbf{x}\|^3} = \partial_{x_3} \frac{x_j}{2\pi\|\mathbf{x}\|^3} \text{ for } j = 1, 2,$$

199 we get for all  $\mathbf{m} = (m_1, m_2, m_3) \in L^2(S, \mathbb{R}^3)$  that

$$b_3[\mathbf{m}] = -\frac{\mu_0}{2} \left( (\partial_{x_1} P_h) \star \widetilde{m}_1 + (\partial_{x_2} P_h) \star \widetilde{m}_2 + (\partial_{x_3} P_{x_3})|_{x_3=h} \star \widetilde{m}_3 \right) \Big|_Q. \quad (8)$$

200 It is easily checked that  $b_3$  is a bounded operator. In fact, being an integral operator  
 201 whose kernel is uniformly continuous on  $S \times Q$ , it is compact [17, Ch. III, Ex. 4.1]. Its  
 202 adjoint  $b_3^* : L^2(Q) \rightarrow L^2(S, \mathbb{R}^3)$  acts on  $\phi \in L^2(Q)$  by the formula

$$b_3^*[\phi] = \frac{\mu_0}{2} \begin{pmatrix} (\partial_{x_1} P_h) \star \widetilde{\phi} \\ (\partial_{x_2} P_h) \star \widetilde{\phi} \\ -(\partial_{x_3} P_{x_3})|_{x_3=h} \star \widetilde{\phi} \end{pmatrix} \Big|_S, \quad (9)$$

203 and is likewise bounded, even compact because so is  $b_3$  [17, Thm 4.10]. A majorization of  
 204 the norm is [5, Sec. 3.3]:

$$\|b_3^*\| \leq b \text{ with } b = \frac{\mu_0}{2} \frac{4\sqrt{2}}{3^{3/2}h}. \quad (10)$$

205 Moreover, by analyticity properties of the Poisson extension, it is not difficult to check  
 206 that  $b_3^*$  is injective whence  $b_3$  has dense range in  $L^2(Q)$  [5, Sec. 3.3].

207 It follows from [7, Thm 2.3] that  $\nabla\Lambda \equiv 0$  on  $\mathbb{R}^3 \setminus S$  if and only if  $m_3 = 0$  and  $(\widetilde{m}_1, \widetilde{m}_2)^t$   
 208 is divergence free on  $\mathbb{R}^2$ , in the distributional sense. Such magnetizations are called silent  
 209 because they generate the zero field outside of their support. Moreover, by [5, Prop. 2],  
 210 it holds that  $b_3[\mathbf{m}] = 0$  if and only if  $\mathbf{m} \vee 0$  is silent. This means that  $m_3 = 0$  and that  
 211  $(m_1, m_2)^t$  belongs to the space  $D_S \subset L^2(S, \mathbb{R}^2)$  consisting of vector fields whose extension  
 212 by zero outside of  $S$  defines a divergence-free vector field on  $\mathbb{R}^2$ . In the proof of [5, Prop.  
 213 2], it is shown that  $D_S$  can be parametrized by Sobolev functions:

$$D_S = \left\{ (-\partial_{x_2} \psi, \partial_{x_1} \psi)^t, \psi \in W_0^{1,2}(S) \right\} \subset L^2(S, \mathbb{R}^2). \quad (11)$$

214 Besides, it follows at once from (11) and the density of  $C_0^\infty(\Omega)$  in  $W_0^{1,2}(\Omega)$  that the  
 215 orthogonal space  $D_S^\perp$  to  $D_S$  in  $L^2(S, \mathbb{R}^2)$  is comprised of those vector fields satisfying the  
 216 distributional Schwarz rule. Since  $S$  is simply connected, these are the distributional  
 217 gradients on  $S$ , by [22, Ch. II, Sec. 6, Thm VI]. Thus, appealing to [12, Thm 6.74] which  
 218 implies that a distribution with  $L^2$  derivative on a Lipschitz open set must be a Sobolev  
 219 function<sup>2</sup>, we conclude that  $D_S^\perp$  is the set  $\nabla W^{1,2}(S)$  of gradients of Sobolev functions.  
 220 Altogether, this leads us to a characterization of the kernel of  $b_3$  and of the range of  $b_3^*$  in  
 221  $L^2(S, \mathbb{R}^3)$  as follows (compare [5, Lem. 4]). If we set  $\mathcal{D}_S = \text{Ker } b_3$ , then

$$\begin{cases} \mathcal{D}_S = \left\{ (-\partial_{x_2} \psi, \partial_{x_1} \psi, 0)^t, \psi \in W_0^{1,2}(S) \right\} \subset L^2(S, \mathbb{R}^3) \text{ and} \\ \mathcal{D}_S^\perp = \overline{\text{Ran } b_3^*} = \overline{b_3^* [W_0^{1,2}(Q)]} = \nabla W^{1,2}(S) \times L^2(S) \subset L^2(S, \mathbb{R}^3), \end{cases} \quad (12)$$

222 where  $\mathcal{D}_S^\perp$  stands for the orthogonal space to  $\mathcal{D}_S$  in  $L^2(S, \mathbb{R}^3)$  and the second equality in  
 223 the second line of (12) holds because  $W_0^{1,2}(Q)$  is dense in  $L^2(Q)$ . Also, rotating pointwise  
 224 by  $\pi/2$  the relation  $D_S^\perp = \nabla W^{1,2}(S)$ , we get that

$$\left[ \nabla W_0^{1,2}(Q) \right]^\perp = \left\{ (-\partial_{x_2} \psi, \partial_{x_1} \psi)^t, \psi \in W^{1,2}(Q) \right\} \subset L^2(Q, \mathbb{R}^2),$$

225 hence vector fields in  $\left[ \nabla W_0^{1,2}(Q) \right]^\perp$  are restrictions to  $S$  of divergence free vector fields in  
 226  $L^2(\mathbb{R}^2, \mathbb{R}^2)$  by the extension theorem for Sobolev functions on a Lipschitz open set [12,  
 227 Prop. 2.70].

### 228 2.3 Moment recovery issues

229 By definition, the net moment  $\langle m_i \rangle$  of the  $i$ -th component  $m_i$  of  $\mathbf{m} \in L^2(S, \mathbb{R}^3)$  is given,  
 230 for  $i = 1, 2, 3$ , by the formula

$$\langle m_i \rangle = \iint_S m_i(\mathbf{t}) \, d\mathbf{t} = \langle \mathbf{m}, \mathbf{e}_i \rangle_{L^2(S, \mathbb{R}^3)}$$

---

<sup>2</sup>The proof given there for bounded  $C^1$ -smooth domains carries over to the Lipschitz case.



231 with  $\mathbf{e}_1 = (\chi_S, 0, 0)^t$ ,  $\mathbf{e}_2 = (0, \chi_S, 0)^t$  and  $\mathbf{e}_3 = (0, 0, \chi_S)^t$ , where  $\chi_S$  denotes the  
 232 characteristic function of  $S$ . Note that  $L^2(S, \mathbb{R}^3) \subset L^1(S, \mathbb{R}^3)$  because  $S$  is bounded, hence  
 233 the above formula for  $\langle m_i \rangle$  makes sense. The net moment  $\langle \mathbf{m} \rangle$  of  $\mathbf{m}$  is simply the vector  
 234  $(\langle m_1 \rangle, \langle m_2 \rangle, \langle m_3 \rangle)^t \in \mathbb{R}^3$ .

235 All magnetizations  $\mathbf{m}'$  such that  $b_3[\mathbf{m}'] = b_3[\mathbf{m}]$  have the same net moment as  $\mathbf{m}$ .  
 236 Indeed,  $b_3[\mathbf{m}] = 0 \Leftrightarrow \mathbf{m} \in \mathcal{D}_S$ , and since  $\mathbf{e}_1, \mathbf{e}_2$  are gradients of Sobolev functions on  $S$   
 237 (namely of  $\mathbf{x} \mapsto x_1, \mathbf{x} \mapsto x_2$ ), we see from (12) that each element of  $\mathcal{D}_S$  is orthogonal to  $\mathbf{e}_i$   
 238 in  $L^2(S, \mathbb{R}^3)$  for  $1 \leq i \leq 3$ . Hence,  $\langle \mathbf{m} \rangle$  is uniquely determined by  $b_3[\mathbf{m}]$ , in other words  
 239 there is a linear map  $\mu : \text{Ran } b_3 \rightarrow \mathbb{R}^3$  such that  $\mu(b_3[\mathbf{m}]) = \langle \mathbf{m} \rangle$  for  $\mathbf{m} \in L^2(S, \mathbb{R}^3)$ . This  
 240 map, however, is not continuous. Otherwise indeed, it would have a continuous extension  
 241  $L^2(Q) \rightarrow \mathbb{R}^3$  by the Hahn-Banach theorem and thus, to each  $i \in \{1, 2, 3\}$ , there would  
 242 exist  $\phi_i \in L^2(Q)$  such that the quantity

$$\begin{aligned} \langle b_3[\mathbf{m}], \phi_i \rangle_{L^2(Q)} - \langle m_i \rangle &= \langle b_3[\mathbf{m}], \phi_i \rangle_{L^2(Q)} - \langle \mathbf{m}, \mathbf{e}_i \rangle_{L^2(S, \mathbb{R}^3)} \\ &= \langle \mathbf{m}, b_3^*[\phi_i] - \mathbf{e}_i \rangle_{L^2(S, \mathbb{R}^3)} \end{aligned} \quad (13)$$

243 vanishes for all  $\mathbf{m} \in L^2(S, \mathbb{R}^3)$ . But the last term in (13) cannot vanish for all  $\mathbf{m}$  unless  
 244  $\mathbf{e}_i = b_3^*(\phi_i)$ , which is impossible because  $\mathbf{e}_i \notin \text{Ran } b_3^*$  by [5, Lem. 7, (iii)].

245 On the one hand, unboundedness of  $\mu$  entails that the moment recovery problem  
 246 knowing  $b_3[\mathbf{m}]$  is ill-posed, in that small variations of  $b_3[\mathbf{m}]$  in the  $L^2(Q)$ -metric may  
 247 result in large variations of  $\langle \mathbf{m} \rangle$ . On the other hand, the fact that  $\mathbf{e}_i \in \mathcal{D}_S^\perp = \overline{\text{Ran } b_3^*}$   
 248 implies that to each  $\varepsilon > 0$  there is  $\phi_{i,\varepsilon} \in L^2(Q)$  such that  $\|b_3^*[\phi_{i,\varepsilon}] - \mathbf{e}_i\|_{L^2(S, \mathbb{R}^3)} \leq \varepsilon$ . Then,  
 249 computing as in (13), we get that

$$\left| \langle b_3[\mathbf{m}], \phi_{i,\varepsilon} \rangle_{L^2(Q)} - \langle m_i \rangle \right| = \left| \langle \mathbf{m}, b_3^*[\phi_{i,\varepsilon}] - \mathbf{e}_i \rangle_{L^2(S, \mathbb{R}^3)} \right| \leq \varepsilon \|\mathbf{m}\|_{L^2(S, \mathbb{R}^3)}. \quad (14)$$

250 Equation (14) shows we can estimate  $\langle \mathbf{m} \rangle$  with arbitrary relative precision, at least  
 251 in principle, by taking the scalar product of the data  $b_3[\mathbf{m}]$  with some appropriate  
 252 estimator  $\phi_{i,\varepsilon}$ . However we necessarily have that  $\|\phi_{i,\varepsilon}\|_{L^2(Q)} \rightarrow +\infty$  when  $\varepsilon \rightarrow 0$ , otherwise  
 253 taking a weakly convergent subsequence would imply in the limit that  $\mathbf{e}_i \in \text{Ran } b_3^*$ , a  
 254 contradiction. Thus, when making  $\varepsilon$  small in order to improve accuracy of the estimate  
 255  $\langle b_3[\mathbf{m}], \phi_{i,\varepsilon} \rangle_{L^2(Q)}$  for  $\langle m_i \rangle$ , we tend to increase the norm of the estimator  $\phi_{i,\varepsilon}$  which in  
 256 turn amplifies the effect of measurement errors when computing the estimate. This is a  
 257 familiar situation with inverse problems, which calls for a regularization technique to find  
 258 a trade off between accuracy of the estimate and precision in the computation; this trade  
 259 off stands analog, in a deterministic context, to the classical compromise between bias  
 260 and variance from stochastic identification.

261 The regularization method we will use is somewhat dual to the Tychonov-type. Yet,  
 262 instead of bounding the norm of the unknown magnetization,  $\mathbf{m}$ , we will control the  
 263  $W_0^{1,2}(Q)$ -norm of the estimator. The reason for this choice is threefold. First, it makes  
 264 sense to keep the norm of the derivative of the estimator at a low level to prevent  
 265 oscillations, since the latter may spoil the evaluation of the net moment from pointwise  
 266 values of  $b_3^*[\mathbf{m}]$ . Second, designing the estimator so as to vanish on the boundary  $\partial Q$   
 267 puts smaller weight on the values of the field close to  $\partial Q$ , which have poor signal/noise  
 268 ratio because of its rapid decay when the distance to the sample increases. Last but  
 269 not least, constraining the  $W_0^{1,2}(Q)$ -norm of the estimator makes for a relatively simple

270 approximation problem to solve, with a critical point equation of elliptic type showing  
 271 interesting regularity properties.

Hereafter we fix  $\mathbf{e} \in \overline{\text{Ran } b_3^*} \subset L^2(S, \mathbb{R}^3)$ . In connection with net moment estimation,  $\mathbf{e}$  can be any of the  $\mathbf{e}_i$  for  $i \in \{1, 2, 3\}$  and then we are in the generic case where  $\mathbf{e} \notin \text{Ran } b_3^*$ , but perspective will be gained if we discuss the more general case. First, observe in view of (12) that

$$\inf_{\phi \in W_0^{1,2}(Q)} \|b_3^*[\phi] - \mathbf{e}\|_{L^2(S, \mathbb{R}^3)} = 0.$$

272 Second, whenever  $\phi_n \in W_0^{1,2}(Q)$  is such that  $\|b_3^*[\phi_n] - \mathbf{e}\|_{L^2(S, \mathbb{R}^3)} \rightarrow 0$  as  $n \rightarrow \infty$ , then ei-  
 273 ther  $\mathbf{e} \in b_3^*[W_0^{1,2}(Q)]$  or  $\|\nabla \phi_n\|_{L^2(Q, \mathbb{R}^2)} \rightarrow \infty$ . For if  $\|\nabla \phi_n\|_{L^2(Q, \mathbb{R}^2)}$  is bounded, extracting  
 274 a subsequence converging weakly to some  $\phi \in W_0^{1,2}(Q)$  and using that the restriction map  
 275  $b_3^* : W_0^{1,2}(Q) \rightarrow L^2(S, \mathbb{R}^3)$  is *a fortiori* continuous, by the Sobolev-Poincaré inequality (2),  
 276 gives us in the limit that  $\mathbf{e} = b_3^*(\phi)$ .

277 To recap, we see from (12) that the quantity

$$\left| \langle b_3[\mathbf{m}], \phi \rangle_{L^2(Q)} - \langle \mathbf{m}, \mathbf{e}_i \rangle_{L^2(S, \mathbb{R}^3)} \right| \leq \|b_3^*[\phi] - \mathbf{e}_i\|_{L^2(S, \mathbb{R}^3)} \|\mathbf{m}\|_{L^2(S, \mathbb{R}^3)} \quad (15)$$

can be made arbitrarily small for appropriate  $\phi$ , but if  $\mathbf{e} \notin b_3^*[W_0^{1,2}(Q)]$  this is at the cost of letting  $\|\nabla \phi\|_{L^2(Q, \mathbb{R}^2)}$  grow unbounded. In practice, one really measures  $b_3[\mathbf{m}] + n$  where  $n$  is some noise (deterministic or stochastic) and thus, we compute  $\langle b_3[\mathbf{m}] + n, \phi \rangle_{L^2(Q)}$  rather than  $\langle b_3[\mathbf{m}], \phi \rangle_{L^2(Q)}$ . If the noise is treated in a deterministic fashion, a relevant estimate is not (15) but

$$\begin{aligned} & \left| \langle b_3[\mathbf{m}] + n, \phi \rangle_{L^2(Q)} - \langle \mathbf{m}, \mathbf{e}_i \rangle_{L^2(S, \mathbb{R}^3)} \right| \\ & \leq \|b_3^*[\phi] - \mathbf{e}_i\|_{L^2(S, \mathbb{R}^3)} \|\mathbf{m}\|_{L^2(S, \mathbb{R}^3)} + \|n\|_{L^2(Q)} \|\phi\|_{L^2(Q)}. \end{aligned}$$

278 So, given *a priori* bounds on  $\|\mathbf{m}\|_{L^2(S, \mathbb{R}^3)}$  and  $\|n\|_{L^2(S)}$ , minimizing the worst case error  
 279 means to minimize the sum of the two terms in the last inequality above. The solution  
 280 to the extremal problem studied in the forthcoming sections offers a tool to trade off  
 281 between them.

### 282 3 A bounded extremal problem

283 We consider the following bounded extremal problem (BEP for short):

284 *Given  $\mathbf{e} \in \overline{\text{Ran } b_3^*} \subset L^2(S, \mathbb{R}^3)$  and a real number  $M > 0$ ,*

285

286 BEP: *find  $\phi_{\text{opt}} \in W_0^{1,2}(Q)$  with  $\|\nabla \phi_{\text{opt}}\|_{L^2(Q, \mathbb{R}^2)} \leq M$  such that*

$$\min_{\phi \in W_0^{1,2}(Q), \|\nabla \phi\|_{L^2(Q, \mathbb{R}^2)} \leq M} \|b_3^*[\phi] - \mathbf{e}\|_{L^2(S, \mathbb{R}^3)} = \|b_3^*[\phi_{\text{opt}}] - \mathbf{e}\|_{L^2(S, \mathbb{R}^3)}.$$

#### 287 3.1 Well posedness

288 **Proposition 1** *There exists a unique solution  $\phi_{\text{opt}}$  to BEP; whenever  $\mathbf{e} \notin b_3^*[W_0^{1,2}(Q)]$ ,*  
 289 *the constraint is saturated:  $\|\nabla \phi_{\text{opt}}\|_{L^2(Q, \mathbb{R}^2)} = M$ .*

290 *Proof:* Since  $\|\nabla\phi\|_{L^2(Q,\mathbb{R}^2)}$  is a norm equivalent to  $\|\phi\|_{W_0^{1,2}(Q)}$  on  $W_0^{1,2}(Q)$  by (3), the  
 291 convex set

$$\{\phi \in W_0^{1,2}(Q), \|\nabla\phi\|_{L^2(Q,\mathbb{R}^2)} \leq M\}$$

292 is weakly compact in the Hilbert space  $W_0^{1,2}(Q)$ . Then, since  $b_3^* : W_0^{1,2}(Q) \rightarrow L^2(S, \mathbb{R}^3)$  is  
 293 continuous hence also weakly continuous [8, Thm 3.10], the set of approximants

$$\mathcal{C} = b_3^* \left[ \{\phi \in W_0^{1,2}(Q), \|\nabla\phi\|_{L^2(Q,\mathbb{R}^2)} \leq M\} \right] \quad (16)$$

294 is weakly compact in  $L^2(S, \mathbb{R}^3)$ . In particular it is weakly closed, and *a fortiori* it is closed  
 295 in the norm topology. This implies there exists a unique best approximation to  $\mathbf{e}$  from  
 296 the closed convex set  $\mathcal{C}$ , that can be written  $b_3^*[\phi_{\text{opt}}]$  for some  $\phi_{\text{opt}} \in W_0^{1,2}(Q)$  which is  
 297 unique because  $b_3^*$  is injective. This ensures both existence and uniqueness of the solution  
 298  $\phi_{\text{opt}}$  to BEP.

299 Next, assume that  $\|\nabla\phi_{\text{opt}}\|_{L^2(Q,\mathbb{R}^2)} < M$ . In this case, the minimum value of the  
 300 criterion is achieved at  $\phi_{\text{opt}}$  which lies interior to the approximation set. We then get by  
 301 differentiating  $\|b_3^*[\phi] - \mathbf{e}\|_{L^2(S,\mathbb{R}^3)}^2$  with respect to  $\phi \in W_0^{1,2}(Q)$  at  $\phi_{\text{opt}}$  that

$$\langle b_3^*[\phi_{\text{opt}}] - \mathbf{e}, b_3^*[\delta_\phi] \rangle_{L^2(S,\mathbb{R}^3)} = \langle b_3 b_3^*[\phi_{\text{opt}}] - b_3[\mathbf{e}], \delta_\phi \rangle_{L^2(Q)} = 0, \quad \forall \delta_\phi \in W_0^{1,2}(Q). \quad (17)$$

302 Hence  $b_3 b_3^*[\phi_{\text{opt}}] - b_3[\mathbf{e}]$  is orthogonal to  $W_0^{1,2}(Q)$  in  $L^2(Q)$ , so by the density of  $W_0^{1,2}(Q)$   
 303 in  $L^2(Q)$  we must have that  $b_3 b_3^*[\phi_{\text{opt}}] - b_3[\mathbf{e}] = 0$ . Thus,  $b_3^*[\phi_{\text{opt}}] - \mathbf{e}$  belongs to  
 304  $\mathcal{D}_S = \text{Ker } b_3$ . However, both  $b_3^*[\phi_{\text{opt}}]$  and  $\mathbf{e}$  belong to  $\mathcal{D}_S^\perp$ , see (12), thus  $b_3^*[\phi_{\text{opt}}] - \mathbf{e} = 0$   
 305 and consequently  $\mathbf{e} = b_3^*[\phi_{\text{opt}}] \in b_3^*[W_0^{1,2}(Q)]$ . This contradicts the assumption on  $\mathbf{e}$ ,  
 306 thereby achieving the proof.  $\square$

307 **Remark 1** *The above proof shows that the constraint is saturated even if  $\mathbf{e} = b_3^*[\phi]$  for*  
 308 *some  $\phi \in W_0^{1,2}(Q)$ , provided that  $\|\nabla\phi\|_{L^2(Q,\mathbb{R}^2)} \geq M$ .*

309

310 **Remark 2** *It follows from the compactness of  $b_3^* : W_0^{1,2}(Q) \rightarrow L^2(S, \mathbb{R}^3)$  that the set  $\mathcal{C}$*   
 311 *defined in (16) is not just closed but actually compact in  $L^2(S, \mathbb{R}^3)$ . This furnishes another*  
 312 *proof of the existence of  $\phi_{\text{opt}}$ , independent of convexity, which can be useful to deal with*  
 313 *additional, possibly non-convex constraints in BEP. However, we do not consider such*  
 314 *generalizations here.*

## 315 3.2 The critical point equation

316 Let  $\phi_{\text{opt}}$  be the solution to BEP whose existence and uniqueness was proven in the previous  
 317 section. Being the projection of  $\mathbf{e}$  onto the closed convex set  $\mathcal{C} \subset L^2(S, \mathbb{R}^3)$ , the vector  
 318 field  $b_3^*[\phi_{\text{opt}}]$  is characterized by the variational inequality [8, Thm 5.2]:

$$\langle \mathbf{e} - b_3^*[\phi_{\text{opt}}], b_3^*[\phi] - b_3^*[\phi_{\text{opt}}] \rangle_{L^2(S,\mathbb{R}^3)} \leq 0, \quad \forall \phi \in W_0^{1,2}(Q), \|\nabla\phi\|_{L^2(Q,\mathbb{R}^2)} \leq M. \quad (18)$$

319 As we deal here with smooth constrained optimization, we can derive a more specific  
 320 critical point equation (in short: CPE) to characterize  $\phi_{\text{opt}}$ . The CPE can be used to  
 321 design numerical algorithms, and it also shows that  $\phi_{\text{opt}}$  is pointwise more regular than  
 322 should *a priori* be expected from a  $W_0^{1,2}(Q)$ -function, namely it is Hölder continuous of  
 323 exponent  $1/2$ . This substantiates a previous claim that constraining the derivative has a  
 324 smoothing effect on our net moment estimator.

325 **Proposition 2** Let  $\mathbf{e} \in \overline{\text{Ran} b_3^*} \setminus b_3^* [W_0^{1,2}(Q)] \subset L^2(S, \mathbb{R}^3)$  and  $M > 0$ .

326 *i)* A function  $\phi_{\text{opt}} \in W_0^{1,2}(Q)$  is the solution to BEP if and only if  $\|\nabla \phi_{\text{opt}}\|_{L^2(Q, \mathbb{R}^2)} = M$   
 327 and there exists  $\lambda > 0$  such that the following critical point equation holds, in the  
 328 distributional sense on  $Q$ :

$$b_3 b_3^* [\phi_{\text{opt}}] - \lambda \Delta \phi_{\text{opt}} = b_3 [\mathbf{e}]. \quad (19)$$

329 *ii)* The function  $\phi_{\text{opt}}$  lies in  $C^\infty(Q)$ , and in the fractional Sobolev space  $W^{3/2,2}(Q)$ , as  
 330 well as in  $C^{1/2}(\overline{Q})$ .

331 *Proof:* If we let  $B : W_0^{1,2}(Q) \rightarrow L^2(Q, \mathbb{R}^2)$  be defined as  $B(\phi) = \nabla \phi$ , then  $\phi_{\text{opt}}$  minimizes  
 332 over  $\phi \in W_0^{1,2}(Q)$  the quantity  $\|b_3^*[\phi] - \mathbf{e}\|_{L^2(S, \mathbb{R}^3)}$  subject to  $\|B(\phi)\|_{L^2(Q, \mathbb{R}^2)} \leq M$ . Now, *i)*  
 333 follows from [9, Thm 2.1] if we identify  $BB^*(\phi)$  with the distribution  $-\Delta \phi$ , which is  
 334 possible since  $C_0^\infty(Q)$  is dense in  $W_0^{1,2}(Q)$ . It is also instructive to establish (19) directly,  
 335 using differentiation. For this, let  $\mathcal{M} \subset W_0^{1,2}(Q)$  be the smooth hypersurface comprised of  
 336 those  $\phi$  such that  $\|\nabla \phi\|_{L^2(Q, \mathbb{R}^2)} = M$ . The tangent space  $T\mathcal{M}_\phi$  to  $\mathcal{M}$  at  $\phi$  is the kernel of  
 337 the linear form on  $W_0^{1,2}(Q)$  given by  $\psi \mapsto \langle \nabla \phi, \nabla \psi \rangle_{L^2(Q, \mathbb{R}^2)}$ . From Proposition 1 we know  
 338 that  $\phi_{\text{opt}} \in \mathcal{M}$  and, by optimality of  $\phi_{\text{opt}}$ , the derivative of  $\phi \mapsto \|b_3^*[\phi] - \mathbf{e}\|_{L^2(S, \mathbb{R}^3)}^2$  at  
 339  $\phi_{\text{opt}}$  must vanish on  $T\mathcal{M}_{\phi_{\text{opt}}}$ . Differentiating as we did in the proof of Proposition 1 and  
 340 expressing that two linear forms with the same kernel must be proportional, we deduce  
 341 there exists  $\lambda \in \mathbb{R}$  such that, for every  $\psi \in W_0^{1,2}(Q)$ ,

$$\langle b_3^*[\phi_{\text{opt}}] - \mathbf{e}, b_3^*[\psi] \rangle_{L^2(S, \mathbb{R}^3)} + \lambda \langle \nabla \phi_{\text{opt}}, \nabla \psi \rangle_{L^2(Q, \mathbb{R}^2)} = 0. \quad (20)$$

342 Clearly we get an equivalent equation upon restricting  $\psi$  in (20) to range over  $C_0^\infty(Q)$ , by  
 343 density of the latter in  $W_0^{1,2}(Q)$ . Thus, by the Green formula for Sobolev functions, we  
 344 find that (20) is equivalent to

$$\langle b_3 b_3^*[\phi_{\text{opt}}] - b_3[\mathbf{e}], \psi \rangle_{L^2(Q)} - \lambda \langle \Delta \phi_{\text{opt}}, \psi \rangle_{L^2(Q)} = 0, \quad \forall \psi \in C_0^\infty(Q),$$

345 which means precisely that (19) holds in the distributional sense. To see that  $\lambda > 0$ ,  
 346 substitute  $\psi = \phi_{\text{opt}}$  in (20) to obtain:

$$\langle b_3^*[\phi_{\text{opt}}] - \mathbf{e}, b_3^*[\phi_{\text{opt}}] \rangle_{L^2(S, \mathbb{R}^3)} = -\lambda \|\nabla \phi_{\text{opt}}\|_{L^2(Q, \mathbb{R}^2)}^2 = -\lambda M^2, \quad (21)$$

347 and observe from (18), with  $\phi = 0$ , that the above quantity is non-positive hence  $\lambda \geq 0$ .  
 348 Moreover  $\lambda \neq 0$ , otherwise (20) would imply that (17) is satisfied and then, arguing as in  
 349 the proof of Proposition 1, it would entail that  $\mathbf{e} \in b_3^* [W_0^{1,2}(Q)]$ , a contradiction.

350 Conversely, assume that  $\|\nabla \phi_{\text{opt}}\|_{L^2(Q, \mathbb{R}^2)} = M$  and that (19) holds for some  $\lambda > 0$ .  
 351 Then Equation (20) holds as well, and so does Equation (21) which is a special case  
 352 of (20). Subtracting (21) from (20), we get that,  $\forall \psi \in W_0^{1,2}(Q)$ ,

$$\langle b_3^*[\phi_{\text{opt}}] - \mathbf{e}, b_3^*[\psi] - b_3^*[\phi_{\text{opt}}] \rangle_{L^2(S, \mathbb{R}^3)} = -\lambda \left( \langle \nabla \phi_{\text{opt}}, \nabla \psi \rangle_{L^2(Q, \mathbb{R}^2)} - M^2 \right),$$

353 and by the Cauchy-Schwarz inequality we find that (18) holds when  $\|\nabla \psi\|_{L^2(Q, \mathbb{R}^2)} \leq M$ .  
 354 Hence  $\phi_{\text{opt}}$  is indeed the solution to BEP, thereby proving *i)*.

355 As to point *ii*), let  $\alpha = (\alpha_1, \alpha_2)$  be a multi-index and set  $\partial^\alpha$  to mean  $\partial_{x_1}^{\alpha_1} \partial_{x_2}^{\alpha_2}$ . Since  
356 distributional derivatives commute, we see from (19) that  $h := \Delta \partial^\alpha \phi_{\text{opt}}$  *a fortiori* belongs  
357 to  $L^2(Q)$  because elements of the range of  $b_3$  are restrictions to  $\overline{Q}$  of real analytic functions  
358 on  $\mathbb{R}^2$ . Now, if we let  $p(z) = -\int_Q \log |z-t| h(t) dt$  be the logarithmic potential of  $\chi_Q h$ , we  
359 have that  $\Delta p = \chi_Q h$  and it is a standard consequence of the Calderón-Zygmund theory  
360 that  $p \in W^{2,2}(\mathbb{R}^2)$  [2, Thm 4.5.3]. Then,  $\partial^\alpha \phi_{\text{opt}} - p$  is harmonic hence real analytic in  $Q$ ,  
361 implying that the restriction of  $\partial^\alpha \phi_{\text{opt}}$  to any relatively compact disk  $D$  in  $Q$  lies in  
362  $W^{2,2}(D)$ . Since  $\alpha$  was arbitrary and  $W^{2,2}(D)$  consists of continuous functions on  $D$  by  
363 the Sobolev embedding theorem [12, Ch. 4], we get that  $\phi_{\text{opt}} \in C^\infty(Q)$ .

364 Finally, as  $\phi_{\text{opt}} \in W_0^{1,2}(Q)$  by definition, it has zero trace on the boundary of the  
365 bounded and Lipschitz-smooth domain  $Q$ , and since  $\Delta \phi_{\text{opt}} \in L^2(Q)$  it follows from [16,  
366 Thm B, 2.] that  $\phi_{\text{opt}}$  belong to  $W^{3/2,2}(Q)$ . By the fractional version of the Sobolev  
367 embedding theorem, it follows that  $\phi_{\text{opt}} \in W^{1,4}(Q)$  and consequently, by the standard  
368 Sobolev embedding theorem, it holds that  $\phi_{\text{opt}} \in C^{1/2}(\overline{Q})$ .  $\square$

369

370 **Remark 3** *The restriction to exponent 3/2 made in point ii) on the Sobolev smoothness*  
371 *of  $\phi_{\text{opt}}$  is due to singularities that may occur on the Lipschitz boundary  $\partial Q$ . For instance*  
372 *if  $\partial Q$  is  $C^\infty$ -smooth, then by elliptic regularity theory we get that  $\phi_{\text{opt}}$  is  $C^\infty$ -smooth on*  
373  *$\overline{Q}$ , for  $\Delta \phi_{\text{opt}}$  is real analytic there and  $\phi_{\text{opt}}$  vanishes on  $\partial Q$ , see [21].*

374 We mention in passing that another application of [9, Thm 2.1] to the solution of extremal  
375 problems for harmonic gradients may be found in [3, Prop. 4].

## 376 4 Analysis of the CPE and resolution schemes

### 377 4.1 Dependence on the constraint and the Lagrange parameter

378 The easiest way to make use of (19) is to pick  $\lambda > 0$  and to solve for  $\phi_{\text{opt}}$ . This can be  
379 done in several manners, two of which will be discussed in this section. However, we  
380 no longer have control on the level of constraint  $M = \|\nabla \phi_{\text{opt}}\|_{L^2(Q, \mathbb{R}^2)}$  when doing this.  
381 This is why we need to know more about the behavior of  $\phi_{\text{opt}}$  and  $M$  as functions of  
382  $\lambda$ . Hereafter, we use  $\phi_{\text{opt}}(\lambda)$  and  $M(\lambda) = \|\nabla \phi_{\text{opt}}(\lambda)\|_{L^2(Q, \mathbb{R}^2)}$  when we want to make the  
383 dependence on  $\lambda$  explicit.

384 **Lemma 1** *Let the assumptions be as in Proposition 2. In (19), the following three*  
385 *statements are equivalent:*

- 386 *i) the level of constraint  $M(\lambda)$  tends to  $+\infty$ ;*
- 387 *ii) the criterion  $\|b_3^*[\phi_{\text{opt}}(\lambda)] - \mathbf{e}\|_{L^2(S, \mathbb{R}^3)}$  tends to 0;*
- 388 *iii) the Lagrange parameter  $\lambda$  tends to 0.*

389 *Moreover,  $M(\lambda)$  is strictly decreasing as a function of  $\lambda$ , and  $M(\lambda) \rightarrow 0$  when  $\lambda \rightarrow +\infty$ .*  
390 *Both  $\phi_{\text{opt}}(\lambda)$  and  $M(\lambda)$  are  $C^\infty$ -smooth functions of  $\lambda \in (0, +\infty)$ , with values in  $W_0^{1,2}(Q)$*   
391 *and  $\mathbb{R}^+$  respectively.*

392 As an illustration, let us mention that the curves obtained numerically in Section 5 and  
 393 shown in Figures 2 and 3 provide a good overview of the properties listed in the lemma.

394

395 *Proof:*

396 *i) ⇒ ii):* Assume that  $M \rightarrow +\infty$ . Since  $\mathbf{e} \in \overline{b_3^* [W_0^{1,2}(Q)]}$ , the minimizing property of  
 397  $\phi_{\text{opt}}$  ensures that  $\|b_3^* [\phi_{\text{opt}}] - \mathbf{e}\|_{L^2(S, \mathbb{R}^3)} \rightarrow 0$ .

398 *ii) ⇒ iii):* if  $\|b_3^* [\phi_{\text{opt}}] - \mathbf{e}\|_{L^2(S, \mathbb{R}^3)} \rightarrow 0$ ,  $\|\phi_{\text{opt}}\|_{L^2(Q)}$  cannot become small since  $\mathbf{e} \neq 0$   
 399 and  $b_3^*$  is continuous. Now, observe that

$$\|\Delta\phi_{\text{opt}}\|_{L^2(Q)} \|\phi_{\text{opt}}\|_{L^2(Q)} \geq |\langle \Delta\phi_{\text{opt}}, \phi_{\text{opt}} \rangle_{L^2(Q)}| = M^2 \geq \frac{1}{C^2} \|\phi_{\text{opt}}\|_{L^2(Q)}^2$$

400 by the Cauchy-Schwarz inequality, the Green formula and the Poincaré-Sobolev inequality.

401 Therefore,  $\|\Delta\phi_{\text{opt}}\|_{L^2(Q)}$  cannot become small either. Because (19) implies that

$$\lambda \|\Delta\phi_{\text{opt}}\|_{L^2(Q)} = \|b_3 [b_3^* [\phi_{\text{opt}}] - \mathbf{e}]\|_{L^2(Q)} \leq \|b_3\| \|b_3^* [\phi_{\text{opt}}] - \mathbf{e}\|_{L^2(S, \mathbb{R}^3)}$$

402 it necessarily holds that  $\lambda \rightarrow 0$ .

403 *iii) ⇒ i):* assume that  $\lambda \rightarrow 0$  but nevertheless  $M = \|\nabla\phi_{\text{opt}}\|_{L^2(Q, \mathbb{R}^2)} \not\rightarrow \infty$ . Then,  
 404 there exists a sequence  $\lambda_k \rightarrow 0$  for which  $M(\lambda_k)$  is bounded, and we see from (20) that

$$\left| \langle b_3^* [\phi_{\text{opt}}(\lambda_k)] - \mathbf{e}, b_3^* [\psi] \rangle_{L^2(S, \mathbb{R}^3)} \right| \rightarrow 0, \quad \forall \psi \in W_0^{1,2}(Q).$$

405 This implies that  $b_3^* [\phi_{\text{opt}}(\lambda_k)]$  converges weakly to  $\mathbf{e}$  in  $L^2(S, \mathbb{R}^3)$ : indeed, consider  
 406  $\Gamma \in L^2(S, \mathbb{R}^3)$  and an arbitrary  $\varepsilon > 0$ ; we decompose  $\Gamma$  as  $\Gamma = \Gamma_{\parallel} + \Gamma_{\perp}$  where  $\Gamma_{\parallel} \in \mathcal{D}_S$  and  
 407  $\Gamma_{\perp} \in \mathcal{D}_S^{\perp}$ . Since  $b_3^* [W_0^{1,2}(Q)]$  is dense in  $\mathcal{D}_S^{\perp} = \overline{\text{Ran } b_3^*}$  by (12), there exists  $\psi \in W_0^{1,2}(Q)$   
 408 such that  $\|b_3^* [\psi] - \Gamma_{\perp}\|_{L^2(S, \mathbb{R}^3)} \leq \varepsilon / \|\mathbf{e}\|_{L^2(S, \mathbb{R}^3)}$  and hence:

$$\begin{aligned} |\langle b_3^* [\phi_{\text{opt}}(\lambda_k)] - \mathbf{e}, \Gamma \rangle_{L^2(S, \mathbb{R}^3)}| &\leq |\langle b_3^* [\phi_{\text{opt}}(\lambda_k)] - \mathbf{e}, \Gamma_{\perp} - b_3^* [\psi] \rangle_{L^2(S, \mathbb{R}^3)}| \\ &\quad + |\langle b_3^* [\phi_{\text{opt}}(\lambda_k)] - \mathbf{e}, \Gamma_{\parallel} \rangle_{L^2(S, \mathbb{R}^3)}| \\ &\quad + |\langle b_3^* [\phi_{\text{opt}}(\lambda_k)] - \mathbf{e}, b_3^* [\psi] \rangle_{L^2(S, \mathbb{R}^3)}| \\ &\leq \varepsilon + |\langle b_3^* [\phi_{\text{opt}}(\lambda_k)] - \mathbf{e}, b_3^* [\psi] \rangle_{L^2(S, \mathbb{R}^3)}|, \end{aligned}$$

409 where we applied that  $\|b_3^* [\phi_{\text{opt}}] - \mathbf{e}\|_{L^2(S, \mathbb{R}^3)} \leq \|\mathbf{e}\|_{L^2(S, \mathbb{R}^3)}$  (because 0 is a candidate  
 410 approximant) together with the Cauchy-Schwarz inequality to bound the first term, and  
 411 we used the fact that  $b_3^* [\phi_{\text{opt}}] - \mathbf{e}$  belongs to  $\mathcal{D}_S^{\perp}$  (cf. proof of Proposition 1), hence is  
 412 orthogonal to  $\Gamma_{\parallel}$  so that the second summand in the middle term of the inequality is zero.  
 413 Finally, for  $k$  large enough (depending only on  $\Gamma$  and  $\varepsilon$ ), the last term is smaller than  $\varepsilon$ ,  
 414 which proves the announced weak convergence.

415 Now, rearranging (21) as

$$\|b_3^* [\phi_{\text{opt}}(\lambda_k)] - \mathbf{e}\|_{L^2(S, \mathbb{R}^3)}^2 = -\langle b_3^* [\phi_{\text{opt}}(\lambda_k)] - \mathbf{e}, \mathbf{e} \rangle_{L^2(S, \mathbb{R}^3)} - \lambda_k M^2(\lambda_k),$$

416 we find since  $\lambda_k M^2(\lambda_k) \rightarrow 0$  by assumption and  $\langle b_3^* [\phi_{\text{opt}}(\lambda_k)] - \mathbf{e}, \mathbf{e} \rangle_{L^2(S, \mathbb{R}^3)} \rightarrow 0$  by the  
 417 weak convergence just proven that  $\|b_3^* [\phi_{\text{opt}}(\lambda_k)] - \mathbf{e}\|_{L^2(S, \mathbb{R}^3)} \rightarrow 0$ . But  $\mathbf{e} \notin b_3^* [W_0^{1,2}(Q)]$   
 418 by hypothesis, therefore this limiting relation implies that  $M(\lambda_k) \rightarrow +\infty$ , as indicated at  
 419 the end of Section 2.3. This contradiction achieves the proof of the first assertion.

To prove that  $\lambda \mapsto \phi_{\text{opt}}(\lambda)$  is smooth, we introduce the operator  $T : L^2(Q) \rightarrow W_0^{1,2}(Q)$  that maps  $\psi \in L^2(Q)$  to the solution  $u \in W_0^{1,2}(Q)$  of the distributional equation  $\Delta u = \psi$ . To see that  $T$  is well-defined, let us introduce the bilinear form  $a_0$  defined for  $u, v \in W_0^{1,2}(Q)$  by  $a_0(u, v) = \langle \nabla u, \nabla v \rangle_{L^2(Q, \mathbb{R}^2)}$ . By density of  $W_0^{1,2}(Q)$  in  $L^2(Q)$ , the equation  $\Delta u = \psi$  holds if and only if  $\langle \Delta u, v \rangle_{L^2(Q)} = \langle \psi, v \rangle_{L^2(Q)}$  for all  $v \in W_0^{1,2}(Q)$ , which is equivalent (thanks to the Green formula) to  $a_0(u, v) = \langle -\psi, v \rangle_{L^2(Q)}$ . Now, the form  $a_0$  is continuous and coercive by Equation (3), therefore the Lax-Milgram theorem (*cf.* [8, Cor. 5.8]) ensures the existence and uniqueness of a solution  $T(\psi) := u \in W_0^{1,2}(Q)$ . Notice, using successively the Cauchy-Schwarz inequality and Equation (2), that

$$\|\nabla u\|_{L^2(Q, \mathbb{R}^2)}^2 = |a_0(u, u)| = \left| \langle -\psi, u \rangle_{L^2(Q)} \right| \leq \|\psi\|_{L^2(Q)} \|u\|_{L^2(Q)} \leq C \|\psi\|_{L^2(Q)} \|\nabla u\|_{L^2(Q, \mathbb{R}^2)},$$

420 whence  $\|\nabla u\|_{L^2(Q, \mathbb{R}^2)} \leq C \|\psi\|_{L^2(Q)}$ . Using Equation (3) we see that  $\|T(\psi)\|_{W^{1,2}(Q)} =$   
 421  $\|u\|_{W^{1,2}(Q)}$  is bounded by  $C \sqrt{C^2 + 1} \|\psi\|_{L^2(Q)}$ , which shows that  $T$  is indeed continuous  
 422 from  $L^2(Q)$  to  $W_0^{1,2}(Q)$ .

423 More in fact is true, as hinted at in the proof of Proposition 2, namely  $T$  maps contin-  
 424 uously  $L^2(Q)$  into  $W_0^{3/2,2}(Q) \subset W_0^{1,2}(Q)$ . This is really the meaning of [16, Thm B, 2.],  
 425 which says in our notation: “if  $\psi \in L^2(\Omega)$ , then  $u \in W^{3/2,2}(\Omega)$ ”. Still, it seems difficult to  
 426 reference an explicit statement, or even a formal argument. As explained in [16, p. 165],  
 427 and also in the proof of Proposition 2, point *ii*), the logarithmic potential  $p$  of  $\chi_Q \psi$   
 428 satisfies  $\Delta p = \psi$  in  $\Omega$  and meets an estimate of the form  $\|p\|_{W^{2,2}(\Omega)} \leq c \|\psi\|_{L^2(Q)}$ , but  
 429 its trace on the boundary  $\partial\Omega$  is not zero. Hence,  $u$  is obtained by subtracting from  $p$   
 430 a harmonic function in  $W^{1,2}(\Omega)$  whose trace is the same as the trace of  $p$ . The latter  
 431 is easily checked to lie in  $W^{1,2}(\partial\Omega)$  (defining Sobolev spaces on Lipschitz manifolds is  
 432 possible because Lipschitz changes of variable preserve Euclidean Sobolev spaces, *cf.* [26,  
 433 Thm 2.2.2]), therefore one is left to prove that a harmonic function  $u \in W^{1,2}(\Omega)$  with  
 434 trace  $\theta \in W^{1,2}(\partial\Omega)$  satisfies  $\|u\|_{W^{3/2,2}(\Omega)} \leq c' \|\theta\|_{W^{1,2}(\partial\Omega)}$  when  $\Omega$  is Lipschitz smooth.  
 435 This may be seen by combining the estimate [11, Eq. (1.1)], putting  $\Phi(x) = x^2$  therein  
 436 and integrating on  $\partial\Omega$ , with [16, Thm 4.1] which gives an equivalent quantity for the  
 437  $W^{3/2,2}(\Omega)$ -norm of a harmonic function. This last reference assumes the dimension is at  
 438 least 3, but the planar case (which is our concern here) may be treated in the same way.  
 439 The result we need is also explicitly stated and formally proved in [4, Prop. 5.2], which  
 440 deals exclusively with dimension 2 (but more general equations). To sum up,  $T$  is not  
 441 just continuous but also compact  $L^2(Q) \rightarrow W_0^{1,2}(Q)$ , by compactness of the embedding  
 442  $W_0^{3/2,2}(Q) \rightarrow W_0^{1,2}(Q)$ , see [12, Thm 4.54].

443 We now turn to the proof that  $\lambda \mapsto \phi_{\text{opt}}(\lambda)$  is smooth. To this end, we first rewrite  
 444 (19) in the form  $F(\lambda, \phi_{\text{opt}}) = 0$  with  $F : \mathbb{R}^+ \times W_0^{1,2}(Q) \rightarrow W_0^{1,2}(Q)$  given by

$$F(\lambda, \phi) = \phi - \frac{T(b_3 b_3^*[\phi]) - T(b_3[e])}{\lambda}, \quad (22)$$

445 Differentiating (22) with respect to  $\phi$ , which is possible since it is affine in  $\phi$ , we get that  
 446  $D_\phi F(\lambda, \phi) = I - T b_3 b_3^* / \lambda$ , where  $I$  denotes the identity operator. Now,  $T b_3 b_3^* : W_0^{1,2}(Q) \rightarrow$   
 447  $W_0^{1,2}(Q)$  is the composition of four operators, namely the embedding  $W_0^{1,2}(Q) \rightarrow L^2(Q)$ ,  
 448 the operator  $b_3^*$ , the operator  $b_3$  and the operator  $T$ . Therefore  $T b_3 b_3^*$  is compact, for it is  
 449 enough to reach the conclusion that one of these operators be compact, whereas all of  
 450 them are! Being a compact perturbation of the identity,  $D_\phi F(\lambda, \phi)$  will be invertible if

451 only it is injective by a classical result of F. Riesz, see *e.g.* [25, Ch. XVII, Prop. 2.3].  
 452 It is indeed injective at every argument  $(\lambda, \phi)$  (note that it does not depend on  $\phi$ ), for  
 453 if  $u \in W_0^{1,2}(Q)$  satisfies  $Tb_3b_3^*[u] = \lambda u$  then we get from the Green formula, and since  
 454  $\Delta u \in L^2(Q)$ , that

$$-\|\nabla u\|_{L^2(Q, \mathbb{R}^2)}^2 = \langle \Delta u, u \rangle_{L^2(Q)} = \lambda^{-1} \langle b_3b_3^*[u], u \rangle_{L^2(Q)} = \lambda^{-1} \|b_3^*[u]\|_{L^2(S, \mathbb{R}^3)}^2$$

455 which implies  $\nabla u = 0$  since the first term is non-positive and the last one non-negative,  
 456 hence also  $u = 0$  by (2). In particular  $D_\phi F(\lambda, \phi_{\text{opt}}(\lambda))$  is an isomorphism of  $W_0^{1,2}(Q)$  for  
 457 each  $\lambda > 0$  and so, by the implicit function theorem in Banach spaces [19, Ch. XIV, Thm  
 458 2.1], we deduce that  $\lambda \rightarrow \phi_{\text{opt}}(\lambda)$  is  $C^\infty$ -smooth on  $\mathbb{R}^+$  since  $F : \mathbb{R}^+ \times W_0^{1,2}(Q) \rightarrow W_0^{1,2}(Q)$   
 459 is obviously smooth. Specifically,  $\phi_{\text{opt}}(\lambda)$  satisfies a linear non-autonomous differential  
 460 equation whose dynamics operator is the resolvent of  $Tb_3b_3^*$ :

$$\frac{d\phi_{\text{opt}}}{d\lambda} = \frac{(\lambda I - Tb_3b_3^*)^{-1}T(b_3[e] - b_3b_3^*[\phi_{\text{opt}}])}{\lambda} = -(\lambda I - Tb_3b_3^*)^{-1}\phi_{\text{opt}}, \quad (23)$$

461 where the first equality holds because  $D_\lambda F(\lambda, \phi_{\text{opt}}(\lambda)) + D_\phi F(\lambda, \phi_{\text{opt}}(\lambda))(d\phi_{\text{opt}}(\lambda)/d\lambda) = 0$   
 462 and the second uses (19) and the fact that  $T\Delta\phi_{\text{opt}} = \phi_{\text{opt}}$  since  $\Delta\phi_{\text{opt}} \in L^2(Q)$ .

463 Next, we observe that for  $u \in W_0^{1,2}(Q)$  with  $u \neq 0$ , the Green formula and the fact  
 464 that  $\Delta T = I$  on  $L^2(Q)$  together imply:

$$\begin{aligned} \langle \nabla(\lambda I - Tb_3b_3^*)u, \nabla u \rangle_{L^2(Q, \mathbb{R}^2)} &= \lambda \|\nabla u\|_{L^2(Q, \mathbb{R}^2)}^2 + \langle \Delta Tb_3b_3^*[u], u \rangle_{L^2(Q)} \\ &= \lambda \|\nabla u\|_{L^2(Q, \mathbb{R}^2)}^2 + \langle b_3b_3^*[u], u \rangle_{L^2(Q)} \\ &= \lambda \|\nabla u\|_{L^2(Q, \mathbb{R}^2)}^2 + \langle b_3^*[u], b_3^*[u] \rangle_{L^2(Q, \mathbb{R}^3)} > 0, \end{aligned}$$

465 and setting  $u = (\lambda I - Tb_3b_3^*)^{-1}v$  gives us

$$\langle \nabla(\lambda I - Tb_3b_3^*)^{-1}v, \nabla v \rangle_{L^2(Q, \mathbb{R}^2)} > 0, \quad \forall v \in W_0^{1,2}(Q), v \neq 0. \quad (24)$$

466 Now, the smoothness of the  $W_0^{1,2}(Q)$ -valued function  $\lambda \mapsto \phi_{\text{opt}}(\lambda)$  entails that  $\lambda \mapsto$   
 467  $\nabla\phi_{\text{opt}}(\lambda)$  is continuously differentiable with values in  $L^2(Q, \mathbb{R}^2)$ , and that  $d(\nabla\phi_{\text{opt}})/d\lambda =$   
 468  $\nabla(d\phi_{\text{opt}}/d\lambda)$ . Thus, it follows from (23) and (24) that

$$\begin{aligned} \frac{dM^2}{d\lambda} &= \frac{d}{d\lambda} \langle \nabla\phi_{\text{opt}}, \nabla\phi_{\text{opt}} \rangle_{L^2(Q, \mathbb{R}^2)} = 2 \langle \nabla \frac{d}{d\lambda} \phi_{\text{opt}}, \nabla\phi_{\text{opt}} \rangle_{L^2(Q, \mathbb{R}^2)} \\ &= -2 \langle \nabla(\lambda I - Tb_3b_3^*)^{-1}\phi_{\text{opt}}, \nabla\phi_{\text{opt}} \rangle_{L^2(Q, \mathbb{R}^2)} < 0, \end{aligned}$$

469 thereby showing that  $M^2(\lambda)$  is smooth and strictly decreasing as a function of  $\lambda$ . Obviously  
 470 the same holds for  $M(\lambda)$ , since it is never zero by the first assumption and the continuity  
 471 of  $\lambda \mapsto M(\lambda)$ . Finally, since  $M(\lambda)$  remains bounded as  $\lambda \rightarrow +\infty$  by the first assertion of  
 472 the lemma (or the monotonicity just proven), it follows from (2) that  $\|\phi_{\text{opt}}\|_{L^2(Q)}$  remains  
 473 bounded as well. Then (19) entails that  $\Delta\phi_{\text{opt}} \rightarrow 0$  in  $L^2(Q)$  as  $\lambda \rightarrow +\infty$ . Applying the  
 474 operator  $T$  now shows that  $\phi_{\text{opt}}(\lambda) \rightarrow 0$  in  $W_0^{1,2}(Q)$  when  $\lambda \rightarrow +\infty$ , hence  $M(\lambda) \rightarrow 0$ .  $\square$

475  
 476 The monotonicity of  $\lambda \mapsto M(\lambda)$  asserted in Lemma 1 provides us with a means to  
 477 approximately solve BEP if we can compute  $\phi_{\text{opt}}(\lambda)$ , because we can use dichotomy on  $\lambda$ .  
 478 Therefore we are reduced to estimate  $\phi_{\text{opt}}(\lambda)$  numerically for fixed  $\lambda$ . It is natural to ask if



479 the fairly explicit differential equation in (23) can be used for this purpose, however several  
480 issues arise in this connection. For instance the obvious boundary condition is  $\phi_{\text{opt}}(\lambda) \rightarrow 0$   
481 in  $W_0^{1,2}(Q)$  when  $\lambda \rightarrow +\infty$ , but the dynamics is singular at infinity. Moreover, integrating  
482 backwards with respect to  $\lambda$  is unstable. In addition, the equation is infinite-dimensional  
483 and a natural basis in which to truncate  $\phi_{\text{opt}}$  consists of eigenvectors of  $Tb_3b_3^*$ , which seem  
484 hardly accessible. In the forthcoming sections, we illustrate how the previous results can  
485 be used to derive a net moment estimator, but we rely on a direct approach based on  
486 numerical integration of (19).

## 487 4.2 Local moments

488 For  $S'$  an open set in  $\mathbb{R}^2$  such that  $\overline{S'} \subset S$ , we define the local moment of the magnetization  
489  $\mathbf{m}$  on  $S'$  to be  $\langle \mathbf{m} \rangle_{S'} = \int_{S'} \mathbf{m}$ . For magnetizations with a density like those considered  
490 in this paper (*i.e.*  $\mathbf{m} \in L^2(S, \mathbb{R}^3)$  in our case), recovering the local moment on any disk  
491  $D(a, r)$  is tantamount to recovering  $\mathbf{m}$  because by Lebesgue's monotone convergence  
492 theorem  $\langle \mathbf{m} \rangle_{D(a,r)} / (\pi r^2) \rightarrow \mathbf{m}(a)$  for a.e.  $a \in S$  when  $r \rightarrow 0$ . Hence it is clear from  
493 the outset that local moments cannot be recovered from the field in general, otherwise  
494 it would contradict the existence of nonzero silent magnetizations. Still the situation is  
495 more nuanced than it seems, and worth a short discussion.

496 First, since vector fields in  $L^2(S, \mathbb{R}^3)$  with vanishing horizontal component are orthog-  
497 onal to  $\mathcal{D}_S$ , by (12), we may set  $\mathbf{e} = (0, 0, \chi_{S'})^t \in \mathcal{D}_S^\perp$  in BEP and the results we obtained  
498 so far apply to any  $S'$ . Thus, the numerical procedures described in sections to come  
499 can be used in principle to estimate the local moments of the vertical component of  $\mathbf{m}$ .  
500 This is consistent with the fact that compactly supported silent magnetizations have null  
501 vertical component.

502 The situation for the vector fields  $(\chi_{S'}, 0, 0)^t$  and  $(0, \chi_{S'}, 0)^t$  is different, for they do  
503 not belong to  $\mathcal{D}_S^\perp$ . However, if  $V$  is an open neighborhood of  $\overline{S'}$  such that  $\overline{V} \subset S$ , there  
504 exists a  $C^1$ -smooth function  $\varphi$  on  $S$  which is identically 1 on  $\overline{S'}$  and 0 on  $S \setminus V$ . Then,  
505 the functions  $\psi_1(x_1, x_2) = \varphi(x_1, x_2)x_1$  and  $\psi_2(x_1, x_2) = \varphi(x_1, x_2)x_2$  are supported in  $V$   
506 and lie in  $W_0^{1,2}(S)$ , so the gradients  $\nabla\psi_1, \nabla\psi_2$  do lie in  $\mathcal{D}_S^\perp$  and they coincide respectively  
507 with  $(\chi_{S'}, 0, 0)^t$  and  $(0, \chi_{S'}, 0)^t$  on  $S'$ . Now, if  $\partial S'$  does not intersect the support of  $\mathbf{m}$ ,  
508 by compactness of the latter we can pick  $V$  to contain no points of  $\text{supp } \mathbf{m}$  except those  
509 contained in  $S'$ , and then  $\int_S \nabla\psi_i \cdot \mathbf{m} = \langle m_i \rangle_{S'}$  for  $i = 1, 2$ . That is to say, if we know  
510 an open set  $S'$  with  $\overline{S'} \subset S$  whose boundary does not intersect  $\text{supp } \mathbf{m}$  (which means of  
511 course we have some *a priori* knowledge on  $\mathbf{m}$ ), we can construct an estimator of the  
512 local moment  $\langle \mathbf{m} \rangle_{S'}$ .

513 In another connection, whereas  $(\chi_{S'}, 0, 0)^t$  and  $(0, \chi_{S'}, 0)^t$  do not belong to  $\mathcal{D}_S^\perp$ , their  
514 projections  $\tilde{\mathbf{e}}_{1,S'}$  and  $\tilde{\mathbf{e}}_{2,S'}$  onto that space in  $L^2(S, \mathbb{R}^3)$  can be taken to be  $\mathbf{e}$  in BEP. Then,  
515 by (12) and the definition of the orthogonal projection, solving this BEP will provide us  
516 with an estimator of the local moment on  $S'$  of the magnetization of minimum  $L^2(S, \mathbb{R}^3)$ -  
517 norm which produces the same field as  $\mathbf{m}$ . Note that  $\tilde{\mathbf{e}}_{1,S'}$  and  $\tilde{\mathbf{e}}_{2,S'}$  can be computed from  
518 the Hodge decomposition of  $(\chi_{S'}, 0, 0)^t$  and  $(0, \chi_{S'}, 0)^t$  by solving a Neumann problem,  
519 identical to the one set up in the proof of [5, Prop. 5].

520 Local moment estimation is a natural extension of our method and has important  
521 practical applications. However, a detailed analysis on this topic is outside the scope of  
522 this paper and will be addressed in a future work.

### 523 4.3 Solving procedures

524 Equation (19) has a unique solution  $\phi_{\text{opt}} \in W_0^{1,2}(Q)$  given  $\mathbf{e} \in L^2(S, \mathbb{R}^3)$  and  $\lambda > 0$ .  
 525 Indeed, taking the scalar product with an arbitrary  $\psi \in W_0^{1,2}(Q)$ , we may use the Green  
 526 formula to obtain the equivalent equation:

$$a_b(\psi, \phi_{\text{opt}}) = \langle \psi, b_3[\mathbf{e}] \rangle_{L^2(Q)}, \quad \forall \psi \in W_0^{1,2}(Q), \quad (25)$$

527 where the bilinear form  $a_b$  on  $[W_0^{1,2}(Q)]^2$  is defined for  $\phi, \psi \in W_0^{1,2}(Q)$  by:

$$a_b(\psi, \phi) = \langle b_3^*[\psi], b_3^*[\phi] \rangle_{L^2(S, \mathbb{R}^3)} + \lambda \langle \nabla \psi, \nabla \phi \rangle_{L^2(Q, \mathbb{R}^2)}.$$

528 Observing that

$$\lambda \|\nabla \phi\|_{L^2(Q, \mathbb{R}^2)}^2 \leq \|b_3^*[\phi]\|_{L^2(S, \mathbb{R}^3)}^2 + \lambda \|\nabla \phi\|_{L^2(Q, \mathbb{R}^2)}^2 \leq b^2 \|\phi\|_{L^2(Q, \mathbb{R}^2)}^2 + \lambda \|\nabla \phi\|_{L^2(Q, \mathbb{R}^2)}^2$$

529 where  $b$  is the bound defined at Equation (10) we see that  $a_b$  is continuous and coercive:

$$c_b \|\phi\|_{W_0^{1,2}(Q)}^2 \leq a_b(\phi, \phi) \leq C_b \|\phi\|_{W_0^{1,2}(Q)}^2$$

530 where we can take, *e.g.*,  $c_b := \lambda/(C^2 + 1)$  and  $C_b := \max(b^2, \lambda)$ , with  $C$  the constant of the  
 531 Sobolev-Poincaré inequality associated to  $Q$  (*cf.* Equation (2)). Therefore, appealing to the  
 532 Lax-Milgram theorem [8, Cor. 5.8], Equation (25) admits a unique solution  $\phi_{\text{opt}} \in W_0^{1,2}(Q)$ .  
 533 Under the additional assumption that  $\mathbf{e} \in \overline{\text{Ran } b_3^*} \setminus b_3^*[W_0^{1,2}(Q)] \subset L^2(S, \mathbb{R}^3)$ , Proposition 2  
 534 tells us that  $\phi_{\text{opt}}$  coincides with the solution of BEP corresponding to the level of constraint  
 535  $M = \|\nabla \phi_{\text{opt}}\|_{L^2(Q, \mathbb{R}^2)}$ .

536 A standard approach to numerically solve equations like (25) is to estimate the solutions  
 537 in weak form, in a space  $V$  of finite dimension. So, let  $(\psi_i)_{i \in I}$  be a finite family of functions<sup>3</sup>  
 538 spanning a subspace  $V = \text{Span}\{\psi_i, i \in I\}$  of  $W_0^{1,2}(Q)$ . Instead of Equation (25), we  
 539 consider the restricted equation

$$a_b(\psi, \phi) = \langle \psi, b_3[\mathbf{e}] \rangle_{L^2(Q)}, \quad \forall \psi \in V, \quad (26)$$

540 where the solution  $\phi$  is searched in the space  $V$ :  $\phi = \sum_{j \in I} \alpha_j \psi_j$  for some real-valued  
 541 coefficients  $(\alpha_j)_{j \in I}$ . Considering Equation (26) with  $\psi = \psi_i$  for every  $i \in I$  then yields  
 542 the system  $\mathcal{A} \alpha = \left( \langle \psi_i, b_3[\mathbf{e}] \rangle_{L^2(S, \mathbb{R}^3)} \right)_{i \in I}$  where  $\mathcal{A} = \mathcal{A}(\lambda)$  is the matrix with coefficients

$$\mathcal{A}_{i,j} = a_b(\psi_i, \psi_j), \quad i, j \in I. \quad (27)$$

543 Solving this system yields the coefficients of the solution  $\phi \in V$  of Equation (26), which,  
 544 by construction, is such that  $a_b(\phi - \phi_{\text{opt}}, \psi) = 0$  for any  $\psi \in V$ . Letting  $\phi_{\parallel}$  indicate  
 545 the orthogonal projection of  $\phi_{\text{opt}}$  onto  $V$  and  $\phi_{\perp} = \phi_{\text{opt}} - \phi_{\parallel}$  indicate its orthogonal  
 546 complement, we thus get

$$\begin{aligned} |a_b(\phi_{\text{opt}} - \phi, \phi_{\text{opt}} - \phi)| &= |a_b(\phi_{\text{opt}} - \phi, \phi_{\perp} + (\phi_{\parallel} - \phi))| = |a_b(\phi_{\text{opt}} - \phi, \phi_{\perp})| \\ &\leq a_b(\phi_{\text{opt}} - \phi, \phi_{\text{opt}} - \phi)^{1/2} |a_b(\phi_{\perp}, \phi_{\perp})|^{1/2}, \end{aligned}$$

---

<sup>3</sup>For instance, in our examples in Section 5 where we deal with square-shaped  $Q$ , we consider a mesh on  $Q$  with  $P \times P$  points, where  $P$  is a parameter. The set  $I$  then corresponds to  $\{(p, q) \in \mathbb{N}^2, 1 \leq p, q \leq P\}$ , and the functions  $(\psi_i)$  are  $Q_1$  finite elements (see Section 5 for details).

547 where the inequality is obtained by Cauchy-Schwarz theorem applied to the positive  
548 form  $a_b$ . This reduces to  $|a_b(\phi_{\text{opt}} - \phi, \phi_{\text{opt}} - \phi)|^{1/2} \leq |a_b(\phi_{\perp}, \phi_{\perp})|^{1/2}$ , whence, with the  
549 coercivity of  $a_b$ :

$$\|\phi_{\text{opt}} - \phi\|_{W_0^{1,2}(Q)} \leq \sqrt{\frac{C_b}{c_b}} \|\phi_{\perp}\|_{W_0^{1,2}(Q)}.$$

550 Notice that all functions  $v$  in  $V$  satisfy  $\|\phi_{\perp}\|_{W_0^{1,2}(Q)} \leq \|v - \phi_{\text{opt}}\|_{W_0^{1,2}(Q)}$  by Pythagora's  
551 theorem. This irreducible error is inherent in the choice of the finite dimensional space  $V$   
552 for representing an approximate solution. Of course, one needs to ensure *a priori* that  
553  $\|\phi_{\perp}\|_{W_0^{1,2}(Q)}$  is small enough. Typically, the space  $V$  will be controlled by some parameter  
554  $\varepsilon$  such that the distance of any given function to  $V = V_{\varepsilon}$  tends to zero when  $\varepsilon \rightarrow 0$ . In  
555 our examples of Section 5, for instance,  $\varepsilon$  corresponds to the step size of the chosen mesh  
556 grid on  $Q$ .

557 In practice, the overall process is as follows. We fix a value  $\varepsilon > 0$ , so that the dimension  
558 of  $V_{\varepsilon}$  is large while keeping the computational burden acceptable. Since we do not know  
559 the value of the Lagrange parameter  $\lambda$  associated with our desired level of constraint  $M$ ,  
560 we iterate the following procedure, starting with some initial value  $\lambda = \lambda_0 > 0$ : compute  
561 the coefficients  $\alpha_j = \alpha_j(\lambda)$  for  $j \in I$ , together with the corresponding approximation  $\phi$  to  
562  $\phi_{\text{opt}}$ , and the associated constraint level  $\|\nabla \phi\|_{L^2(Q, \mathbb{R}^2)}$ . If the latter is within a satisfactory  
563 range of  $M$ , we stop. Otherwise we bisection with respect to variable  $\lambda$ , according to the rule  
564 indicated by Lemma 1: increasing it when the constraint level is too high, and decreasing  
565 it otherwise.

566 If at some point monotonicity fails numerically, it means that the computations are  
567 inaccurate, *e.g.*, that  $\phi_{\text{opt}}$  is still fairly far from  $V_{\varepsilon}$  (*i.e.*,  $\|\phi_{\perp}\|_{W_0^{1,2}(Q)}$  is fairly large) and  
568 we should try a smaller value of  $\varepsilon$ .

569 The above-described procedure is simple and yields fairly good results on the synthetic  
570 examples reported in Section 5. However, the precision strongly depends on  $\|\phi_{\perp}\|_{W_0^{1,2}(Q)}$   
571 and the computational burden on  $\dim(V_{\varepsilon})$ . It is therefore important to pick a family  
572  $(\psi_i)$  able to approximate  $\phi_{\text{opt}}$  with as few elements as possible, in spite of its oscillatory  
573 behaviour in certain regions that can be guessed from Lemma 1 and confirmed numerically.  
574 For the experiments presented in the next section to illustrate the technique, we did not  
575 try to optimize the design of  $(\psi_i)$  and did favour simplicity. More sophisticated choices of  
576 the basis are left here for further study.

577  
578 The previous approach aims at approximating  $\phi_{\text{opt}}$  in  $W_0^{1,2}(Q)$ -norm but tells us  
579 nothing about pointwise convergence, in particular it does not reflect that  $\phi_{\text{opt}} \in C^{1/2}(\overline{Q})$ ,  
580 see Proposition 2. This is why it seems worth describing another algorithm to solve  
581 Equation (19), which is more demanding computationally in general but offers some  
582 guarantee in this respect. It is based on successive approximations of the CPE itself by  
583 standard Dirichlet problems. More precisely, for  $\mathbf{e} \in L^2(S, \mathbb{R}^3)$ ,  $\lambda > 0$ ,  $\varrho > 0$ ,  $\phi_1 \in W_0^{1,2}(Q)$   
584 and  $n \geq 2$ , we consider the sequence of equations:

$$(I - \varrho \lambda \Delta) \phi_n = (I - \varrho b_3 b_3^*) \phi_{n-1} + \varrho b_3 [\mathbf{e}], \quad (28)$$

585 where  $\phi_n \in W_0^{1,2}(Q)$  is the unknown and  $\phi_{n-1}$  acts as a parameter which was computed  
586 at the previous step.

587 Let us first show that, given  $\phi_{n-1} \in W_0^{1,2}(Q)$ , there exists a unique solution  $\phi_n \in$   
588  $W_0^{1,2}(Q)$  to (28). Indeed, the bilinear form on  $[W_0^{1,2}(Q)]^2$  defined by

$$a(\phi, \psi) = \langle \phi, \psi \rangle_{L^2(Q)} + \varrho \lambda \langle \nabla \phi, \nabla \psi \rangle_{L^2(Q, \mathbb{R}^2)} = \langle (I - \varrho \lambda \Delta) \phi, \psi \rangle_{L^2(Q)}$$

589 is continuous and coercive, while taking the scalar product with an arbitrary  $\psi \in W_0^{1,2}(Q)$   
590 on both sides of (28) yields the equivalent formulation:

$$a(\phi_n, \psi) = \langle (I - \varrho b_3 b_3^*) \phi_{n-1} + \varrho b_3 [e], \psi \rangle_{L^2(Q)}, \quad \forall \psi \in W_0^{1,2}(Q),$$

591 which has a unique solution  $\phi_n \in W_0^{1,2}(Q)$  by the Lax-Milgram theorem.

592 Thus, given some initial  $\phi_1 \in W_0^{1,2}(Q)$ , we can define inductively a sequence of  
593  $W_0^{1,2}(Q)$ -functions  $(\phi_n)_{n \in \mathbb{N}^*}$ , where  $\phi_n$  is the solution to (28) for  $n \geq 2$ .

594 **Proposition 3** *Let  $e \in \overline{\text{Ran } b_3^*} \setminus b_3^* [W_0^{1,2}(Q)] \subset L^2(S, \mathbb{R}^3)$ ,  $\lambda > 0$ , and  $\phi_1 \in W_0^{1,2}(Q)$ .*

595 *i) For  $\varrho > 0$  small enough, (28) defines a sequence of functions  $(\phi_n)$  for  $n \geq 2$  that*  
596 *converges in  $W_0^{1,2}(Q)$  to the unique solution  $\phi_{\text{opt}}(\lambda)$  of the critical point equation (19).*  
597 *In particular  $\|\nabla \phi_n\|_{L^2(Q, \mathbb{R}^2)} \rightarrow M(\lambda)$  as  $n \rightarrow \infty$ .*

598 *ii) Actually,  $\phi_n \in C^{1/2}(\overline{Q})$  for  $n \geq 2$  and  $(\phi_n)$  converges to  $\phi_{\text{opt}}$  in  $C^{1/2}(\overline{Q})$ .*

599 *Proof:* Multiplying (19) by  $\varrho$  and subtracting it from (28), we obtain that

$$(I - \varrho \lambda \Delta) [\phi_n - \phi_{\text{opt}}] = (I - \varrho b_3 b_3^*) [\phi_{n-1} - \phi_{\text{opt}}], \quad (29)$$

600 and taking the scalar product with  $\phi_n - \phi_{\text{opt}}$  in  $L^2(Q)$  yields:

$$\begin{aligned} \|\phi_n - \phi_{\text{opt}}\|_{L^2(Q)}^2 + \varrho \lambda \|\nabla (\phi_n - \phi_{\text{opt}})\|_{L^2(Q, \mathbb{R}^2)}^2 \\ = \langle (I - \varrho b_3 b_3^*) [\phi_{n-1} - \phi_{\text{opt}}], \phi_n - \phi_{\text{opt}} \rangle_{L^2(Q)} \\ \leq \|I - \varrho b_3 b_3^*\| \|\phi_{n-1} - \phi_{\text{opt}}\|_{L^2(Q)} \|\phi_n - \phi_{\text{opt}}\|_{L^2(Q)}. \end{aligned} \quad (30)$$

601 Clearly we may assume that  $\phi_n \neq \phi_{\text{opt}}$  for all  $n \geq 1$ , for if  $\phi_{n_0} = \phi_{\text{opt}}$  it follows from (30)  
602 that  $\phi_n = \phi_{\text{opt}}$  for all  $n \geq n_0$  and there is nothing to prove. Now, using Equation (2) on  
603 the left-hand side and dividing on both sides by  $\|\phi_n - \phi_{\text{opt}}\|$  we get

$$\|\phi_n - \phi_{\text{opt}}\|_{L^2(Q)} \leq \frac{\|I - \varrho b_3 b_3^*\|}{1 + \frac{\varrho \lambda}{C^2}} \|\phi_{n-1} - \phi_{\text{opt}}\|_{L^2(Q)}. \quad (31)$$

604 Next, observe that ( $b$  being the bound introduced with Equation (10))

$$\langle (I - \varrho b_3 b_3^*) \phi, \phi \rangle_{L^2(Q)} = \|\phi\|_{L^2(Q)}^2 - \varrho \|b_3^*[\phi]\|_{L^2(Q)}^2 \geq (1 - \varrho b^2) \|\phi\|_{L^2(Q)}^2. \quad (32)$$

605 Therefore, whenever  $0 < \varrho < 1/b^2$ , the operator  $I - \varrho b_3 b_3^*$  is positive self-adjoint on  $L^2(Q)$ ,  
606 so its norm is (see *e.g.* [8, Prop. 6.9]):

$$\|I - \varrho b_3 b_3^*\| = \sup_{\substack{\phi \in L^2(Q) \\ \|\phi\|_{L^2(Q)} \leq 1}} \langle (I - \varrho b_3 b_3^*) \phi, \phi \rangle_{L^2(Q)},$$

607 which, in view of the equality in (32), is smaller than 1. From (31) we finally obtain

$$\|\phi_n - \phi_{\text{opt}}\|_{L^2(Q)} \leq \kappa \|\phi_{n-1} - \phi_{\text{opt}}\|_{L^2(Q)}, \quad \text{with } \kappa = \frac{1}{1 + \frac{\varrho\lambda}{C^2}} < 1$$

608 which establishes that  $\|\phi_n - \phi_{\text{opt}}\|_{L^2(Q)}$  decreases to 0 geometrically fast as  $n \rightarrow \infty$ .

609 Rewriting now (29) in the form:

$$\phi_n - \phi_{\text{opt}} = \frac{1}{\varrho\lambda} T \left( (\phi_n - \phi_{\text{opt}}) - (I - \varrho b_3 b_3^*) [\phi_{n-1} - \phi_{\text{opt}}] \right) \quad (33)$$

610 where the operator  $T$  was defined in the proof of Lemma 1, we get from [16, Thm B, 2.]  
 611 and the convergence of  $\phi_n - \phi_{\text{opt}}$  to 0 in  $L^2(Q)$  that  $\phi_n - \phi_{\text{opt}}$  also converges to 0 in  
 612  $W_0^{3/2,2}(Q) \subset W_0^{1,2}(Q)$ , thereby proving *i*). Point *ii*) now follows from the embedding  
 613  $W^{3/2,2}(Q) \rightarrow C^{1/2}(\overline{Q})$  pointed out in the proof of Proposition 2, point *ii*).  $\square$

614

615 Still, computing the solution to (28) with good accuracy on pointwise values is not an  
 616 easy task. Let us simply mention that Equation (28) can be rewritten as the equivalent  
 617 equation

$$\phi_n = -T(\varrho\lambda I - T)^{-1} \left( (I - \varrho b_3 b_3^*) [\phi_{n-1}] + \varrho b_3 [\mathbf{e}] \right). \quad (34)$$

An interesting feature of this formulation is that the factor  $T$  has a smoothing effect, converting  $L^2(Q)$ -convergence into  $C^{1/2}(\overline{Q})$ -convergence. Moreover, if  $Q$  is a rectangle, the eigenfunctions and eigenvalues of the Laplacian are explicitly known (the eigenfunctions are products of sines) [18]. They form a Hilbert basis of  $L^2(Q)$  on which the operators  $T$  and  $(\varrho\lambda I - T)^{-1}$  are diagonal. Let us denote with  $(u_{p,q})_{p,q \in \mathbb{N}}$  the eigenfunctions and assume that the expansion of  $\phi_{n-1} = \sum_{p,q \in \mathbb{N}} \beta_{p,q} u_{p,q}$  is known. Thanks to the orthonormality of the basis, the coefficients  $\beta'_{k,l}$  of the expansion of  $(I - \varrho b_3 b_3^*) [\phi_{n-1}]$  in the basis are given by

$$\beta'_{k,l} = \left\langle \sum_{p,q \in \mathbb{N}} \beta_{p,q} (I - \varrho b_3 b_3^*) [u_{p,q}], u_{k,l} \right\rangle_{L^2(Q)} = \beta_{k,l} - \varrho \sum_{p,q \in \mathbb{N}} \beta_{p,q} \langle b_3^* [u_{p,q}], b_3^* [u_{k,l}] \rangle_{L^2(S, \mathbb{R}^3)}.$$

618 Therefore, once the products  $\langle b_3^* [u_{p,q}], b_3^* [u_{k,l}] \rangle_{L^2(S, \mathbb{R}^3)}$  and  $\langle u_{p,q}, b_3 [\mathbf{e}] \rangle_{L^2(Q)}$  have been  
 619 precomputed, it is easy to get the expansion of  $\phi_n$  from the expansion of  $\phi_{n-1}$ . The compu-  
 620 tational burden in the case of a rectangle is overall fairly similar to the first approach, the  
 621 precomputation of  $\langle b_3^* [u_{p,q}], b_3^* [u_{k,l}] \rangle_{L^2(S, \mathbb{R}^3)}$  playing the same role as the precomputation of  
 622 the matrix  $\mathcal{A}$  of Equation (27), and the precomputation of  $\langle u_{p,q}, b_3 [\mathbf{e}] \rangle_{L^2(Q)}$  corresponding  
 623 to the computation of the right-hand side of Equation (26). However, thanks to the  
 624 properties of  $T$ , these expansions do not only converge in  $L^2(Q)$ , but indeed in  $C^{1/2}(\overline{Q})$ ,  
 625 while the first approach approximates  $\phi_{\text{opt}}$  only weakly. A thorough study of the precision  
 626 required in the computation to make the  $C^{1/2}(\overline{Q})$  convergence effective, though, is beyond  
 627 the scope of the present paper.

## 628 5 Numerical aspects and illustrations

629 We ran preliminary numerical experiments on the direct resolution scheme proposed in  
 630 Section 4.3, using a family of finite elements in  $W_0^{1,2}(Q)$ . Observe that Equation (19) is

631 an elliptic partial differential-integral equation to be solved on a square  $Q$ , subject to  
632 a homogeneous Dirichlet boundary condition. We thus make use of a family  $(\psi_{p,q})$  of  
633 bilinear rectangular elements on a square mesh of  $Q$ . These elements are piecewise affine  
634 in the variables  $x_1, x_2$  separately, and are the simplest ones to expand  $W_0^{1,2}(Q)$ -functions  
635 on a rectangle, see [10, Ch. 2] and [13].

## 636 5.1 Details of our implementation

637 **Mesh on  $Q$ .** We choose a number  $P \in \mathbb{N}^*$  that controls the number of elements that  
638 we use to mesh the rectangle  $Q$ . In order to simplify the presentation, we take  $Q$  to  
639 be the square  $[-R, R] \times [-R, R] \times \{h\} \subset \mathbb{R}^2 \times \{h\}$ , and we define  $\delta = 2R/(P+1)$  and  
640  $\kappa_i = -R + i\delta$  for  $i = 1, \dots, P$ , so that the points of coordinates  $(\kappa_p, \kappa_q)$ ,  $1 \leq p, q \leq P$   
641 constitute the  $P \times P$  interior nodes of a square mesh of  $Q$  with step  $\delta$ .

642 We denote with  $Q_{p,q}$  the square centered at the node  $(\kappa_p, \kappa_q)$  with side-length equal  
643 to  $2\delta$  and edges parallel to the axes. Observe that  $Q = \cup_{p,q=1,\dots,P} Q_{p,q}$  but the union is  
644 not disjoint as the squares overlap (a generic  $Q_{p,q}$  shares interior points with its 8 closest  
645 neighbours,  $Q_{p',q'}$  such that  $p' \in \{p-1, p, p+1\}$  and  $q' \in \{q-1, q, q+1\}$ ). This is  
646 illustrated on Figure 1.

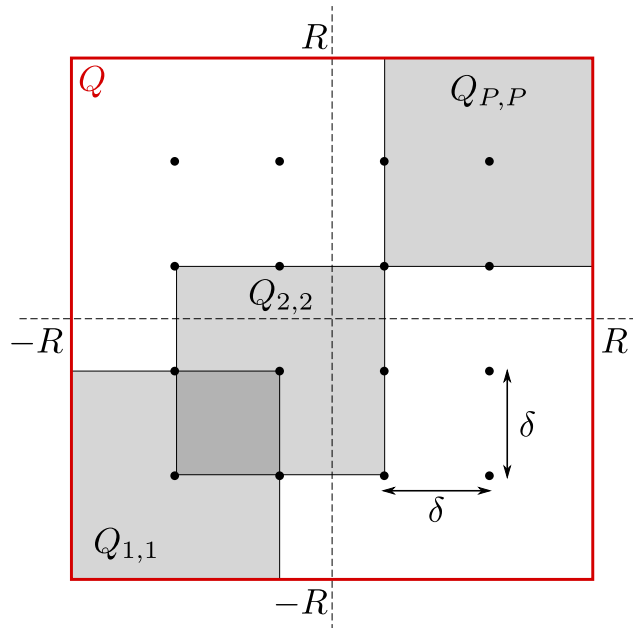


Figure 1: The mesh on  $Q$ , here with  $P = 4$ . The points of coordinates  $(\kappa_p, \kappa_q)$  ( $1 \leq p, q \leq P$ ) are represented by bullets. The elementary squares  $Q_{p,q}$  overlap, as shown in the diagram.

**Elements.** We take for  $p, q = 1, \dots, P$  the  $W_0^{1,2}(Q)$ -functions  $\psi_{p,q}$  defined on  $Q$  by

$$\psi_{p,q}(x_1, x_2) = \left(1 - \frac{|x_1 - \kappa_p|}{\delta}\right) \left(1 - \frac{|x_2 - \kappa_q|}{\delta}\right) \chi_{Q_{p,q}}.$$

By construction, each  $\psi_{p,q}$  is 0 on the boundary and outside  $Q_{p,q}$  (it actually belongs to  $W_0^{1,2}(Q_{p,q}) \subset W_0^{1,2}(Q)$ ) and ranges from 0 to 1 inside  $Q_{p,q}$ , taking value 1 exactly at its

center  $(\kappa_p, \kappa_q)$ . These properties make  $(\psi_{p,q})$  an interpolating family of Lagrange type (the so-called  $\mathbb{Q}_1$  type). In particular, a function  $\phi \in \text{Span}\{\psi_{p,q}\}_{1 \leq p,q \leq P}$ ,

$$\phi = \sum_{1 \leq p,q \leq P} \alpha_{p,q} \psi_{p,q},$$

647 always satisfies  $\phi(\kappa_p, \kappa_q) = \alpha_{p,q}$  for all  $1 \leq p, q \leq P$ . Indeed, if we extend the notations  
 648 by taking  $\kappa_0 = -R$ ,  $\kappa_{P+1} = R$  and  $\alpha_{0,q} = \alpha_{P+1,q} = \alpha_{p,0} = \alpha_{p,P+1} = 0$  for any  $0 \leq p, q \leq$   
 649  $P + 1$ , then  $\phi$  is the unique function whose restriction to any  $[\kappa_p, \kappa_{p+1}] \times [\kappa_q, \kappa_{q+1}]$  (with  
 650  $0 \leq p, q \leq P$ ) is a function of the form  $(x_1, x_2) \mapsto a + bx_1 + cx_2 + dx_1x_2$  (with  $a, b, c,$   
 651 and  $d$  real values depending of course on  $p$  and  $q$ ) and satisfying  $\phi(\kappa_p, \kappa_q) = \alpha_{p,q}$  for any  
 652  $0 \leq p, q \leq P + 1$ .

**Integrals on  $S$ .** For  $S$ , we also take a square, namely  $S = [-s, s] \times [-s, s] \times \{0\} \subset \mathbb{R}^2 \times \{0\}$ . The computations require evaluating a number of integrals on  $S$ : this is done using the trapezoidal rule applied on a uniform  $N \times N$  grid for some parameter  $N \geq 3$ . Specifically, using the notations  $\rho = 2s/(N - 1)$  and  $\sigma_i = -s + i\rho$  for  $i = 0, \dots, N - 1$ , the integral of a function  $f$  on  $S$  is approximated by

$$\iint_S f \simeq \rho^2 \sum_{i=0}^{N-1} \sum_{j=0}^{N-1} w_{i,j} f(\sigma_i, \sigma_j),$$

653 where  $w_{0,0} = w_{0,N-1} = w_{N-1,0} = w_{N-1,N-1} = 1/4$ ,  $w_{0,j} = w_{N-1,j} = w_{i,0} = w_{i,N-1} = 1/2$   
 654 for  $1 \leq i, j \leq N - 2$  and  $w_{i,j} = 1$  otherwise.

**Dot products on  $Q$ .** We occasionally need to compute the dot product of  $L^2(Q)$  between a function  $\phi$  of  $\text{Span}\{\psi_{p,q}\}_{1 \leq p,q \leq P}$  and a smooth function  $g$  defined on  $Q$ . When it happens, we first approximate  $g$  with the elements  $(\psi_{p,q})$ , *i.e.*,

$$g \simeq g_{\text{approx}} = \sum_{1 \leq k,l \leq P} g(\kappa_k, \kappa_l) \psi_{k,l},$$

655 and we then evaluate exactly  $\langle \phi, g_{\text{approx}} \rangle_{L^2(Q)} = \iint_Q \phi g_{\text{approx}}$ . More precisely, if  $\phi =$   
 656  $\sum_{1 \leq p,q \leq P} \alpha_{p,q} \psi_{p,q}$ , we have

$$\langle \phi, g_{\text{approx}} \rangle_{L^2(Q)} = \sum_{1 \leq p,q \leq P} \sum_{1 \leq k,l \leq P} \alpha_{p,q} g(\kappa_k, \kappa_l) \langle \psi_{p,q}, \psi_{k,l} \rangle_{L^2(Q)}. \quad (35)$$

657 Hence, the computation boils down to evaluating a discrete sum. The terms  $\langle \psi_{p,q}, \psi_{k,l} \rangle_{L^2(Q)}$   
 658 are analytically precomputed, once and for all, from the explicitly known expressions of  
 659 the elements  $(\psi_{p,q})$ . Notice that such a product is non-zero only when the interiors of  
 660  $Q_{p,q}$  and  $Q_{k,l}$  overlap and that its value depends only on  $p - k$  and  $q - l$ . Hence there are  
 661 actually only a few integrals to compute.

662 **Computation of the matrix  $\mathcal{A}$ .** In order to construct the matrix from Equation (27),  
 663 we need to compute the dot products  $\langle \nabla \psi_{p,q}, \nabla \psi_{k,l} \rangle_{L^2(Q, \mathbb{R}^2)}$  and  $\langle b_3^*[\psi_{p,q}], b_3^*[\psi_{k,l}] \rangle_{L^2(S, \mathbb{R}^3)}$ .

664 Regarding the former, the gradients  $\nabla \psi_{p,q}$  are explicitly known from the above expres-  
 665 sions for  $\psi_{p,q}$ , so that these products can be analytically computed. The remarks we made  
 666 for the computation of  $\langle \psi_{p,q}, \psi_{k,l} \rangle_{L^2(Q)}$  apply here also.

As to the products  $\langle b_3^*[\psi_{p,q}], b_3^*[\psi_{k,l}] \rangle_{L^2(S, \mathbb{R}^3)}$  they are computed as the sum of three integrals on  $S$ , each one being evaluated by the trapezoidal rule as explained above. This requires to numerically estimate  $b_3^*[\psi_{p,q}](\sigma_i, \sigma_j)$  for all  $1 \leq p, q \leq P$  and  $0 \leq i, j \leq N - 1$ . We do it using Formula (9) with  $\phi = \psi_{p,q}$ : denoting with  $K$  the convolution kernel ( $K = \partial_{x_1} P_h$  or  $K = \partial_{x_2} P_h$  or  $K = (\partial_{x_3} P_{x_3})|_{x_3=h}$  depending on the component being considered), the value of  $(K \star \tilde{\phi})(\sigma_i, \sigma_j)$  is evaluated, with the method described above, as the dot product

$$[K \star \tilde{\phi}](\sigma_i, \sigma_j) = \langle K_{i,j}, \psi_{p,q} \rangle_{L^2(Q)},$$

667 where  $K_{i,j} : (x_1, x_2) \mapsto K(\sigma_i - x_1, \sigma_j - x_2)$ . The numerical evaluations of  $K_{i,j}$  are obtained  
668 by an explicit formula for  $K_{i,j}$  analytically derived from its definition and Equation (6).

669 **Right-hand side of the system.** The right-hand side of Equation (26) requires to  
670 evaluate  $\langle \psi_{p,q}, b_3[e] \rangle_{L^2(Q)}$  for all  $1 \leq p, q \leq P$ . These are dot products on  $Q$  of the form  
671 described above, so we simply need to compute  $b_3[e](\kappa_k, \kappa_l)$  for all  $1 \leq k, l \leq P$ . This is  
672 done using Equation (8): convolutions with the same kernels as before appear, except that  
673 the integrals involved are now on  $S$  and not on  $Q$ . We evaluate them with the trapezoidal  
674 rule described above.

## 675 5.2 Numerical results

676 Numerical simulations were performed using MATLAB. The geometry of the measurement  
677 setup is fixed to  $R = 0.00255$  and  $h = 0.00027$ , while the sample size is  $s = 0.00197$ .  
678 This corresponds to a small, yet realistic, sample studied by SQUID microscopy. The  
679 discretization parameters  $P$  and  $N$  have been chosen to be  $P = N = 100$ .

680 We estimated the solution of the Critical Point Equation (19) using the above-described  
681 algorithm, for different values of  $\lambda$ , and for the right-hand sides corresponding to  $e = e_k$   
682 with  $k = 1$  and  $k = 3$ . We denote with  $\phi_{e_k}(\lambda)$  the approximation of the true solution  
683  $\phi_{\text{opt}}$  so obtained. Notice that the case  $k = 2$  is similar to the case  $k = 1$ , by symmetry  
684 (because  $\phi_{e_2}(x_1, x_2) = \phi_{e_1}(x_2, x_1)$ ), which is why we only show the results corresponding  
685 to  $e_1$  and  $e_3$ . Figures 2 and 3 show how the criterion  $\|b_3^*[\phi_{e_k}(\lambda)] - e_k\|_{L^2(S, \mathbb{R}^3)}$  and the  
686 level of constraint  $M(\lambda) = \|\nabla \phi_{e_k}(\lambda)\|_{L^2(Q, \mathbb{R}^2)}$  depend on  $\lambda$ . This is in accordance with  
687 the assertions of Lemma 1 about the behavior of  $\phi_{\text{opt}}$ .

688 Figure 4 shows the same information in another form by plotting the evolution of the  
689 criterion with respect to the level of constraint. This is the so-called L-curve (see [14]):  
690 when the level of constraint  $M$  is fairly small, the criterion decreases very fast, meaning  
691 that the quality of the linear estimator can be much improved, at the small cost of making  
692 it behave only slightly worse (a small increase of  $M$  intuitively means slightly larger  
693 oscillations of  $\phi_{\text{opt}}$ ). On the other hand, for larger values of  $M$ , the criterion is barely  
694 improved even when  $M$  is rather well increased, meaning that the benefit on the quality of  
695 the linear estimator is not worth the deterioration of its behavior. A compromise between  
696 both situation lies at the “elbow” of the L-curve, *e.g.*, around values of  $M$  corresponding  
697 to  $\lambda = 10^{-21}$  or  $\lambda = 10^{-22}$ .

698 We show on Figure 5 the functions  $\phi_{e_k}(\lambda)$  ( $k = 1$  and  $3$ ) for  $\lambda = 10^{-21}$ . They are  
699 plotted on a rectangle slightly larger than  $Q$  to help understand how they behave at the  
700 boundary of  $Q$  (they are, by definition, equal to 0 outside  $Q$ ). On the bottom layer of



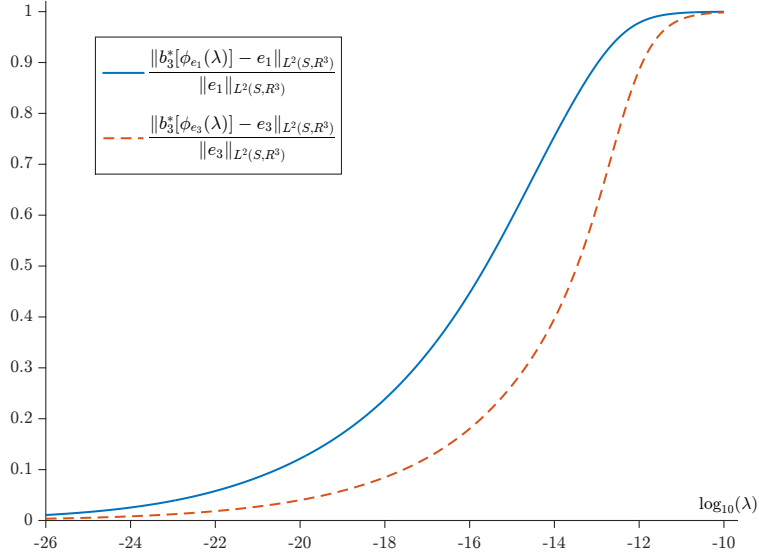


Figure 2: Approximation error of  $b_3^*[\phi_{e_k}(\lambda)]$  with respect to  $e_k$  when  $\lambda$  varies (the scale for  $\lambda$  is logarithmic). The solid line corresponds to the case when  $k = 1$ , while the dashed line corresponds to the case when  $k = 3$ . As expected from Lemma 1, on the one hand, when  $\lambda$  goes to 0 (*i.e.*,  $\log_{10}(\lambda) \rightarrow -\infty$ ), the error tends to 0. On the other hand, when  $\lambda$  goes large, the constraint  $M(\lambda)$  goes to 0, meaning that  $\phi_{\text{opt}}$  is forced to go to 0, whence the relative error tends to 1.

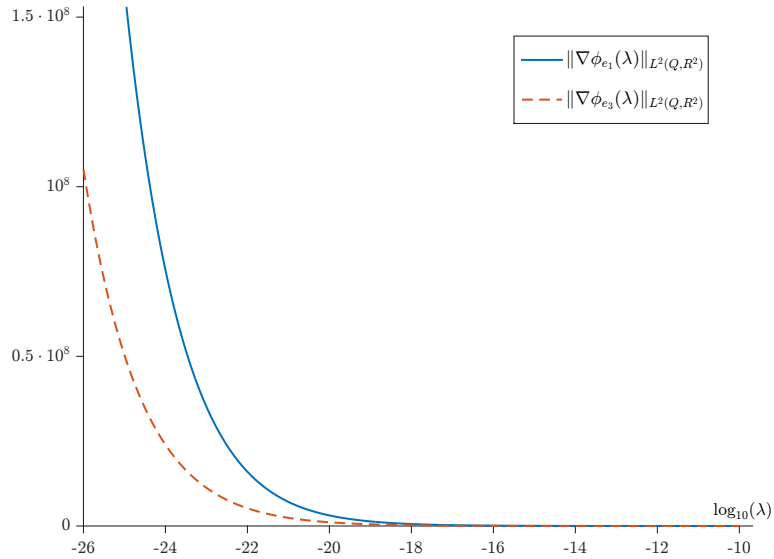


Figure 3: Constraint  $M(\lambda) = \|\nabla\phi_{e_k}(\lambda)\|_{L^2(Q, R^2)}$  as a function of  $\lambda$  (the scale for  $\lambda$  is logarithmic). The solid line corresponds to the case when  $k = 1$ , while the dashed line corresponds to the case when  $k = 3$ . As expected from Lemma 1, these are strictly decreasing smooth functions tending to  $+\infty$  when  $\lambda \rightarrow 0$  (*i.e.*,  $\log_{10}(\lambda) \rightarrow -\infty$ ) and tending to 0 when  $\lambda \rightarrow +\infty$ .

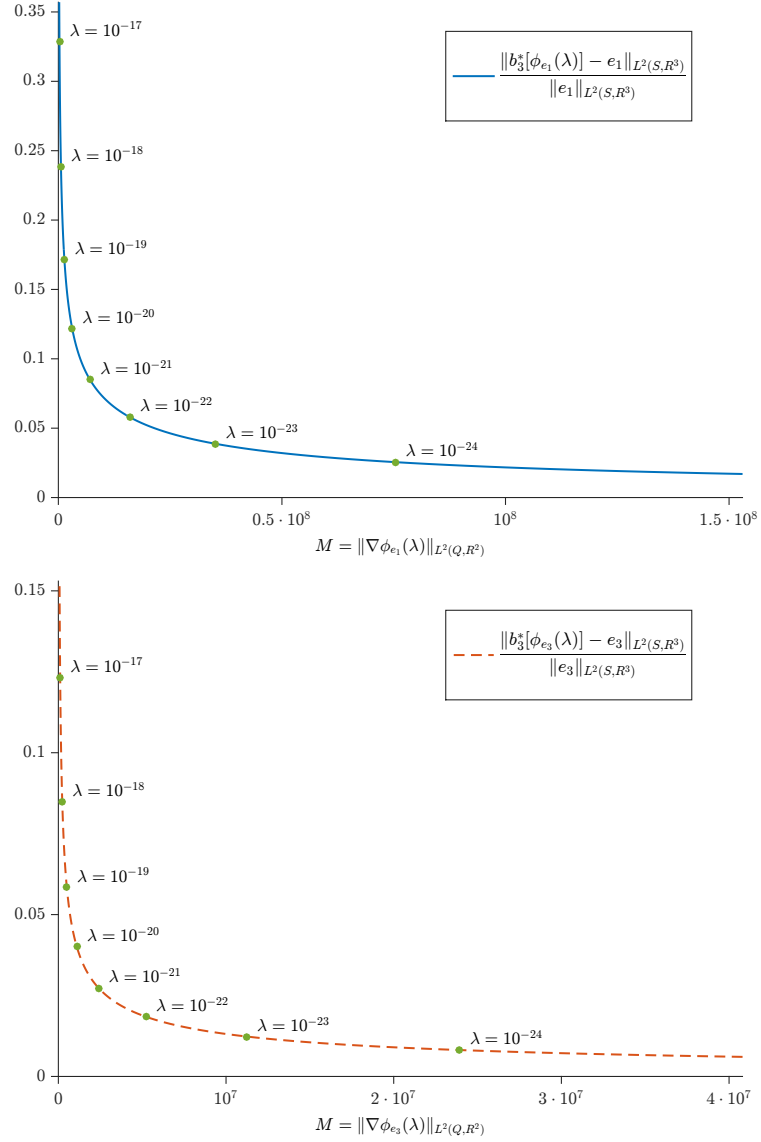


Figure 4: “L-curves” showing the approximation error  $\|b_3^*[\phi_{e_k}(\lambda)] - e_k\|_{L^2(S, \mathbb{R}^3)} / \|e_k\|_{L^2(S, \mathbb{R}^3)}$  as a function of the constraint  $M = \|\nabla\phi_{e_k}(\lambda)\|_{L^2(Q, \mathbb{R}^2)}$ . The upper plot corresponds to the case when  $k = 1$ , and the lower one to the case when  $k = 3$ . As expected, the error decreases and tends to 0 as the constraint is relaxed.

701 each plot, a map is displayed where the color of each pixel corresponds to the value of the  
702 function. This does not say more than the plot itself, but in a complementary way, in  
703 order to help understanding the oscillations pattern of  $\phi_{e_k}$ . Also, on the same bottom  
704 layer, the rectangles  $Q$  and  $S$  are displayed, so as to recall their respective positions. We  
705 can see that the functions  $\phi_{e_k}$  already have a fairly important oscillation pattern when  
706  $\lambda = 10^{-21}$ , more specifically on the region corresponding to  $Q \setminus S$ . Indeed the maximal  
707 absolute value of  $\phi_{e_1}$  on  $Q \setminus S$  is approximately  $6.8 \cdot 10^5$  while its maximal absolute value  
708 on  $S$  is roughly  $0.89 \cdot 10^5$ . The same observation holds for  $\phi_{e_3}$  (with respective values  
709  $1.95 \cdot 10^5$  and  $0.38 \cdot 10^5$ ). Also, we can see that the highest oscillations are close to the  
710 boundary of  $Q$ , and indeed the functions go to 0 fairly abruptly on  $\partial Q$ . This means that,  
711 when estimating the moment  $\langle \mathbf{m} \rangle$  from the data  $b_3[\mathbf{m}]$  with the linear estimator, much  
712 importance will be given to the values of the field measured near the edges, in spite of  
713 the fact that the vanishing of  $\phi_{\text{opt}}$  on  $\partial Q$  was imposed in hope to avoid this issue. The  
714 latter may be a drawback in practice, as measurements taken near the edges usually have  
715 lower signal-to-noise ratios, and further analysis is needed here to check how much this  
716 can affect the results with real data and whether there is a need to devise a remedy.

717 Finally, a close inspection of the plots, especially at some peaks of the functions, seems  
718 to suggest that the functions exhibit kinks and are not very smooth. This is likely to  
719 be an artefact due to the approximation of  $\phi_{\text{opt}}$  by a function in  $\text{Span}\{\psi_{p,q}\}_{1 \leq p,q \leq P}$  and  
720 indicates that the choice of  $P$  might be a bit too small to render the behavior of  $\phi_{\text{opt}}$   
721 accurately at those places.

722 In order to test the ability of the computed estimators  $\phi_{e_k}(\lambda)$  with  $\lambda = 10^{-21}$  to  
723 recover net moments, we considered a synthetic magnetization  $\mathbf{m} = (m_1, m_2, m_3)$  on  $S$ .  
724 The considered magnetization is shown on Figure 6 and is based on the logo of the Apics  
725 project-team. We discretized the logo on a  $540 \times 540$  grid of dipoles. Each part of the  
726 logo (letter A, letters PICS, and mountain) is magnetized along a different direction.  
727 The dipoles belonging to each part have close moments, but not exactly equal, hence  
728 simulating an almost uniformly magnetized shape. Overall, the net moment of the  
729 ‘A’ part is approximately  $(-12, -86, 3.5) \cdot 10^{-6}$ , the net moment of the ‘PICS’ part is  
730 approximately  $(-61, -26, 25) \cdot 10^{-6}$  and the net moment of the mountain is approximately  
731  $(-0.76, -0.28, 13) \cdot 10^{-6}$ . The total net moment  $\langle \mathbf{m} \rangle$  of the synthetic magnetization  
732 is approximately  $(-74, -112, 41) \cdot 10^{-6}$ . The choice of using dipoles does not strictly  
733 match our framework of working with  $L^2$  magnetizations, but the grid is intended to be  
734 fine enough that it might actually be viewed as a practical approximation of a piecewise  
735 continuous magnetization. The reason for this choice is practical: it allows us to simply  
736 use the exact formula for the field of a magnetic dipole in order to evaluate the forward  
737 operator  $b_3$ .

738 We computed the values of  $b_3[\mathbf{m}]$  at the points of our mesh on  $Q$ . To test the influence  
739 of additive noise, we also generated a Gaussian white noise component with a magnitude  
740 of order roughly 1% of the maximal absolute value of  $b_3[\mathbf{m}]$ . Using these values, we  
741 approximated the field and the noise as functions on  $Q$  using the elements  $(\psi_{p,q})$ , in  
742 order to evaluate the dot products with functions  $\phi_{e_k}(\lambda)$  ( $k = 1, 2, 3$ ) as described in  
743 Equation (35). Figure 7 shows the corresponding functions, and Table 1 sums up our  
744 results.

745 In absence of noise, the relative error between the individual components  $\langle m_k \rangle$  and  
746 their estimates decrease as  $\lambda$  tends to 0 because  $b_3[\mathbf{m}]$  is smooth enough that its integral

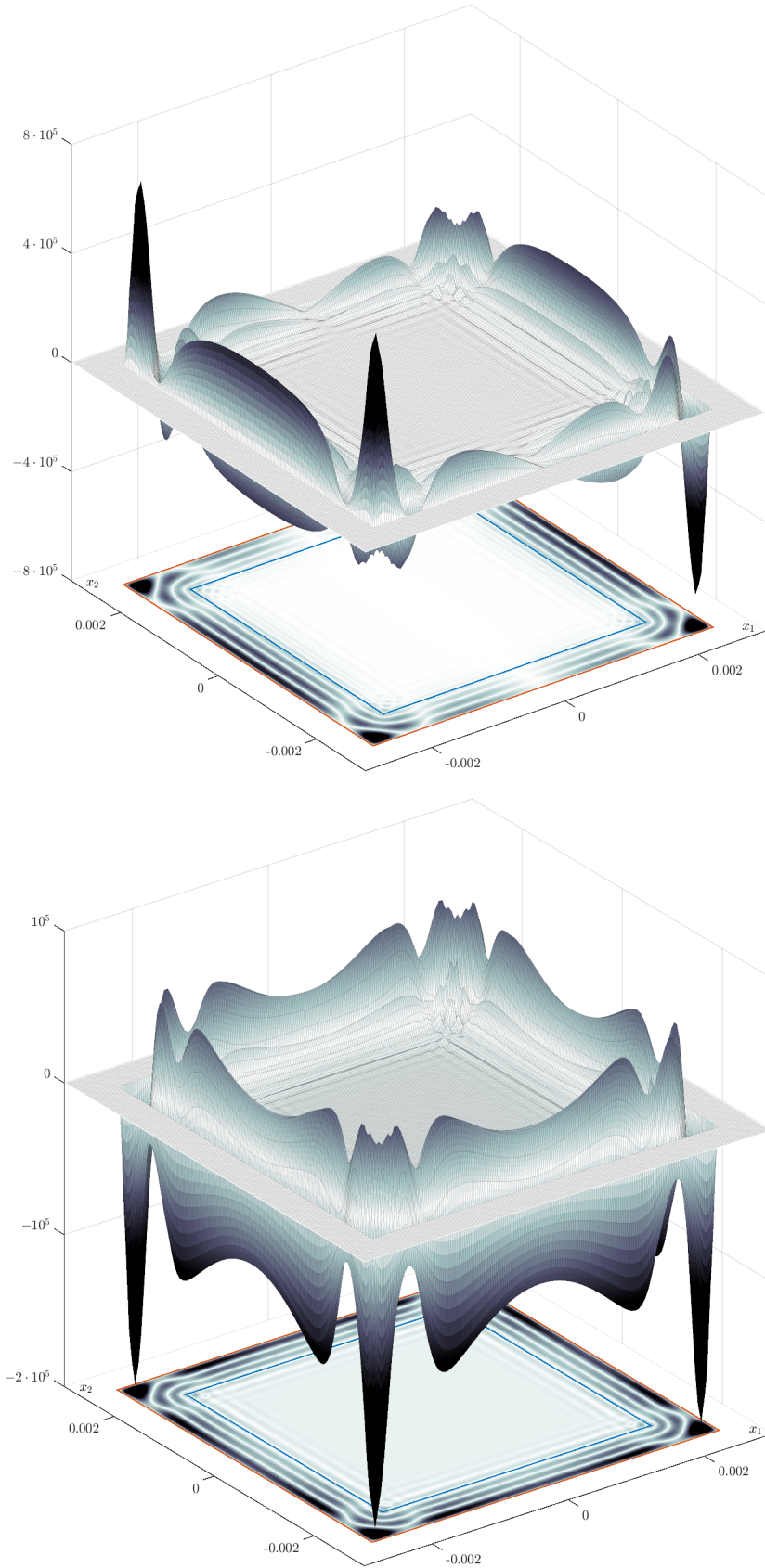


Figure 5:  $\phi_{e_1}(\lambda)$  (top) and  $\phi_{e_3}(\lambda)$  (bottom) for  $\lambda = 10^{-21}$ . On both plots, the rectangles  $Q$  (red) and  $S$  (blue) are drawn together on the bottom layer to help visualize their respective positions.

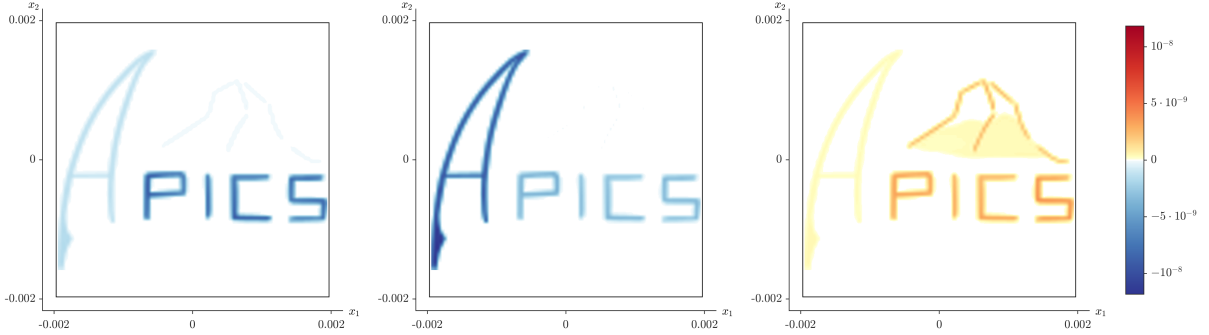


Figure 6: Synthetic magnetization (from left to right)  $m_1$ ,  $m_2$  and  $m_3$  on  $S$ .

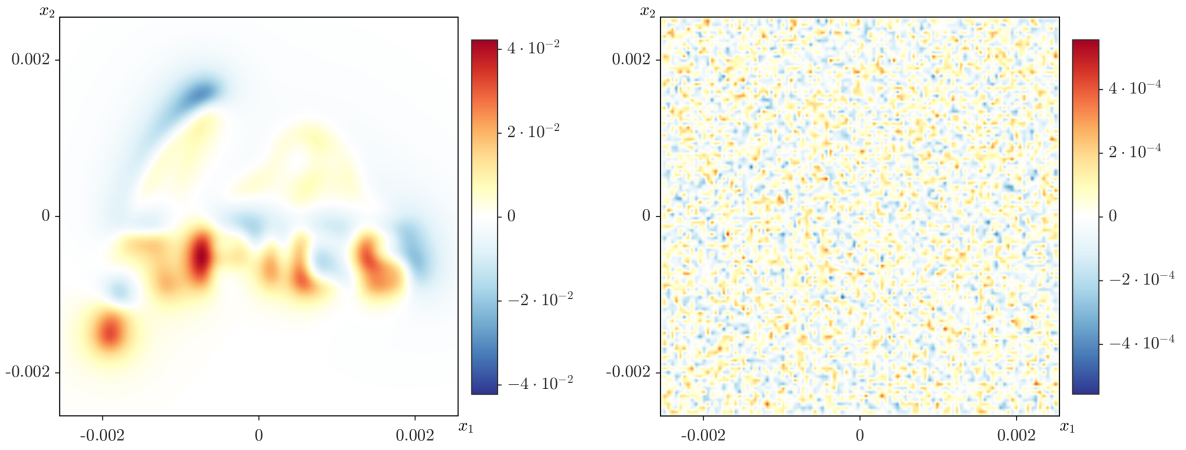


Figure 7: Field  $b_3[m]$  corresponding to the synthetic magnetization shown on Figure 6 and an additive Gaussian white noise generated on the same  $P \times P$  mesh on  $Q$ , with  $P = 100$ . The computed values are used to approximate the field and the noise as functions of  $\text{Span}\{\psi_{p,q}\}_{1 \leq p,q \leq P}$ . Note that the color scales are not the same on both pictures.

747 against the linear estimators  $\phi_{e_k}(\lambda)$  is fairly well evaluated. Interestingly, the component  
748  $\langle m_3 \rangle$  is more accurately recovered than the others, which is likely connected with the  
749 fact that the inverse problem of recovering  $m_3$  from  $b_3[\mathbf{m}]$  has a unique solution (because  
750 silent sources have a null vertical component) whereas recovering  $m_1$  or  $m_2$  does not. This  
751 difference is reflected in the expression of the kernels generating  $\partial_{x_1}\Lambda$  and  $\partial_{x_2}\Lambda$  from  $\mathbf{m}$ ,  
752 compare (5) and (7).

753 In contrast, in the presence of noise, we see that the quality of the estimate is first  
754 getting better as  $\lambda$  decreases, but it reaches an optimum and the error starts increasing  
755 when  $\lambda$  goes below some level because the linear estimators peak so much and oscillate so  
756 fast that their dot product against the noise become non-trivial.

$\lambda$	No noise					With noise	
	$\delta_1$ (%)	$\delta_2$ (%)	$\delta_3$ (%)	$\delta_r$ (%)	$\theta$ (°)	$\delta_r$ (%)	$\theta$ (°)
$10^{-18}$	12.56	14.77	3.02	-13.10	2.13	-12.93	2.28
$10^{-19}$	7.41	9.15	2.08	-8.05	1.23	-7.73	1.33
$10^{-20}$	4.91	5.52	1.61	-5.01	0.65	-4.44	0.70
$10^{-21}$	3.50	3.17	1.25	-3.10	0.34	-0.41	1.03
$10^{-22}$	2.50	1.71	0.95	-1.86	0.26	6.66	2.37
$10^{-23}$	1.71	0.86	0.73	-1.08	0.23	17.87	4.34
$10^{-24}$	1.11	0.38	0.53	-0.59	0.18	31.97	5.76

Table 1: The components  $\langle m_k \rangle$  ( $k = 1, 2, 3$ ) of the net moment  $\langle \mathbf{m} \rangle$  are approximated thanks to the linear estimator as  $\mu_k = \langle b, \phi_{e_k}(\lambda) \rangle_{L^2(Q)}$  for several values of  $\lambda$  and with  $b$  being either the exact synthetic field  $b_3[\mathbf{m}]$  or the exact field plus some noise.

The quantities  $\delta_k$  are the relative errors  $\delta_k = (\mu_k - \langle m_k \rangle) / \langle m_k \rangle$ . The quantity  $\delta_r$  is the relative error of the amplitude of  $\boldsymbol{\mu} = (\mu_1, \mu_2, \mu_3)$  as a vector approximation of  $\langle \mathbf{m} \rangle$ , *i.e.*,  $\delta_r = (\|\boldsymbol{\mu}\| - \|\langle \mathbf{m} \rangle\|) / \|\langle \mathbf{m} \rangle\|$ , where  $\|\cdot\|$  denotes the Euclidean norm. Finally,  $\theta$  is the angle between the vectors  $\boldsymbol{\mu}$  and  $\langle \mathbf{m} \rangle$ , *i.e.*,  $\theta = \frac{360}{2\pi} \arccos\left(\frac{\boldsymbol{\mu} \cdot \langle \mathbf{m} \rangle}{\|\boldsymbol{\mu}\| \cdot \|\langle \mathbf{m} \rangle\|}\right)$ .

## 757 6 Concluding remarks

758 In this paper, we considered the inverse moment problem in magnetostatics, and derived  
759 linear estimators for the moment from the field in a planar geometry, We did this in a  
760 Hilbertian framework for  $L^2$  magnetizations on thin slabs, and we studied a regularization  
761 technique based on the solution of a bounded extremal problem for the estimator. En-  
762 couraging numerical experiments, reported in Section 5, were carried out on a synthetic  
763 though already nontrivial example, with 1% synthetic Gaussian white noise added, using  
764 the simple resolution scheme described in Section 4.3. The treatment of real data by  
765 this method can still be enhanced by using more precise estimates of  $b_3^*[\psi_{p,q}]$  than those  
766 obtained using quadrature formulas, in order to get a more accurate version of the matrix  
767  $\mathcal{A}$  and of the right-hand side in (26). Moreover, finer (possibly adaptive) meshes can be  
768 used, though this will increase the computational burden. An alternating strategy, when  
769 the measurement area is a rectangle, rests on solving Equation (34) in the eigenbasis of  
770 the Laplacian, *cf.* the discussion at the end of Section 4.3.

771 However, when dealing with physical data, we should face additional problems arising  
772 from increased, non purely stochastic noise and other imperfections in the measurements.  
773 We did not touch upon this issue in the present paper whose main focus is theoretical,  
774 with numerical experiments designed for demonstrating the method under moderately  
775 realistic conditions.

776 It would be interesting to carry the approach over to magnetizations modeled by  
777 more general measures than those having  $L^2$ -density, and to more regular (*e.g.*, Lipschitz-  
778 smooth) estimators. This is needed to handle some popular models for magnetizations  
779 such as sums of dipoles. Although the problem looks more difficult, we expect that the  
780 method can be adapted to this case.

781 **Acknowledgements.** All authors were supported in part by an Inria grant to the  
782 associate team IMPINGE. L. Baratchart, S. Chevillard, J. Leblond and E. A. Lima also  
783 acknowledge support from the MIT-France seed fund. The research of D. Hardin and the  
784 research of E. A. Lima were supported, in part, by the U.S. National Science Foundation  
785 under the grants DMS-1521749 and DMS-1521765, respectively. We are grateful to  
786 M. Northington and D. Ponomarev for many valuable discussions.

## 787 References

- 788 [1] R. A. Adams. *Sobolev Spaces*. Academic Press, 1975.
- 789 [2] K. Astala, T. Iwaniec, and G. Martin. *Elliptic Partial Differential Equations and*  
790 *Quasiconformal mappings in the plane*. Princeton Univ. Press, 2009.
- 791 [3] B. Atfeh, L. Baratchart, J. Leblond, and J. R. Partington. Bounded extremal and  
792 Cauchy-Laplace problems on the sphere and shell. *Journal of Fourier Analysis and*  
793 *Applications*, 16(2):177–203, 2010.
- 794 [4] L. Baratchart, L. Bourgeois, and J. Leblond. Uniqueness results for inverse Robin  
795 problems with bounded coefficient. *Journal of Functional Analysis*, 270(7):2508–2542,  
796 2016. <http://dx.doi.org/10.1016/j.jfa.2016.01.011>.
- 797 [5] L. Baratchart, S. Chevillard, and J. Leblond. Silent and equivalent magnetic distribu-  
798 tions on thin plates. To appear in Theta Series in Advanced Mathematics, available  
799 at <http://hal.inria.fr/hal-01286117v2>.
- 800 [6] L. Baratchart, S. Chevillard, J. Leblond, E. A. Lima, and D. Ponomarev. Moments  
801 estimation of magnetic source terms from partial data. In preparation. Preprint  
802 available at <https://hal.inria.fr/hal-01421157/>.
- 803 [7] L. Baratchart, D. P. Hardin, E. A. Lima, E. B. Saff, and B. P. Weiss. Characterizing  
804 kernels of operators related to thin-plate magnetizations via generalizations of Hodge  
805 decompositions. *Inverse Problems*, 29(1), 2013.
- 806 [8] H. Brezis. *Functional Analysis, Sobolev Spaces and Partial Differential Equations*.  
807 Springer, 2011.

- 808 [9] I. Chalendar and J. R. Partington. Constrained approximation and invariant sub-  
809 spaces. *J. Mathematical Analysis and Applications*, 280:176–187, 2003.
- 810 [10] P. Ciarlet. *The finite element method for elliptic problems*. North-Holland, 1980.
- 811 [11] B. Dahlberg. Weighted norm inequality for the Lusin area integral and the non-  
812 tangential maximal functions for functions harmonic in a Lipschitz domain. *Studia*  
813 *Math.*, 67(3):297–314, 1980.
- 814 [12] F. Demengel and G. Demengel. *Espaces fonctionnels, Utilisation dans la résolution*  
815 *des équations aux dérivées partielles*. EDP Sciences/CNRS Editions, 2007.
- 816 [13] A. Ern and J.-L. Guermond. *Theory and Practice of Finite Elements*. Springer, 2004.
- 817 [14] P. C. Hansen. *Rank-Deficient and Discrete Ill-Posed Problems*. SIAM, 1998.
- 818 [15] J. D. Jackson. *Classical Electrodynamics*. J. Wiley & Sons, 3rd edition, 1998.
- 819 [16] D. Jerison and C. E. Kenig. The inhomogeneous Dirichlet problem in Lipschitz  
820 domains. *J. Functional Analysis*, 130:161–219, 1995.
- 821 [17] T. Kato. *Perturbation Theory for Linear Operators*, volume 132 of *Grundlehren der*  
822 *mathematischen wissenschaften*. Springer-Verlag, 2 edition, 1976.
- 823 [18] J. Kuttler and V. Sigillito. Eigenvalues of the Laplacian in two dimensions. *SIAM*  
824 *Review*, 26(2), 1984.
- 825 [19] S. Lang. *Real and functional analysis*. Springer, 3 edition, 1993.
- 826 [20] E. A. Lima, B. P. Weiss, L. Baratchart, D. P. Hardin, and E. B. Saff. Fast inversion  
827 of magnetic field maps of unidirectional planar geological magnetization. *Journal of*  
828 *Geophysical Research: Solid Earth*, 118(6):2723–2752, 2013.
- 829 [21] J. Lions and E. Magenes. *Problèmes aux limites non homogènes et applications*,  
830 volume I. Dunod, Paris, 1968.
- 831 [22] L. Schwartz. *Théorie des distributions*. Hermann, 1966.
- 832 [23] E. M. Stein. *Singular Integrals and Differentiability Properties of Functions*. Princeton  
833 University Press, 1970.
- 834 [24] E. M. Stein and G. Weiss. *Introduction to Fourier analysis on Euclidean spaces*.  
835 Princeton Univeristy Press, 1971.
- 836 [25] A. Torchinsky. *Real-variable Methods in Harmonic Analysis*. Academic Press, San  
837 Diego, 1986.
- 838 [26] W. P. Ziemer. *Weakly Differentiable Functions, Sobolev Spaces and Functions of*  
839 *Bounded Variation*, volume 120 of *Graduate Texts in Mathematics*. Springer-Verlag,  
840 1989.